Gut Microbiome Modifications Ameliorate Chemosensory Deficiencies in *Caenorhabditis elegans* Models of Alzheimer's Disease

A Major Qualifying Project
submitted to the Faculty of
WORCESTER POLYTECHNIC INSTITUTE
in partial fulfillment of the requirements for the
Degree in Bachelor of Science.

By

Sarah Tarantino
Biology & Biotechnology

Submitted on: 12/16/2021
Approved By:

Jagan Srinivasan, PhD
Worcester Polytechnic Institute
Biology & Biotechnology

Abstract

It is estimated that 1 in 9 individuals over the age of 65 are living with Alzheimer's disease (AD) and research has shown that the prevalence rate is growing. Currently there is no cure and only limited treatments for AD. Dysbiosis of the gut microbiome has been observed in patients with AD and may contribute to the development of the disease. This study used a transgenic *Caenorhabditis elegans* AD model to investigate the therapeutic potential of gut microbiome supplementation and punicalagin extract as treatment of AD. Behavioral assays were used to assess the potential amelioration of chemoreception deficiencies of the *C. elegans* AD model with treatment. It was found that gut microbiome supplementation partially improved chemoreception deficiencies and punicalagin treatment fully improved chemoreception to control level. Both of these treatments have potential as acting as therapeutics for AD.

Acknowledgments

I would like to thank all the members of the Srinivasan Lab for their help and support throughout this project. I would especially like to thank Caroline Muirhead, Elizabeth DiLoreto and Annalise Robidoux for their continued support and assistance. I would also like to thank my advisor Dr. Jagan Srinivasan (Dr. J) for his support and guidance.

Table of Contents

1.0 Background

1.1 Alzheimer's Disease

Alzheimer's disease (AD), the most common form of dementia, is currently the 6th leading cause of death in the United States with a prevalence rate of 37 cases per 100,000 people (Centers for Disease Control [CDC], 2019; CDC, 2021a). AD is a progressive neurodegenerative disease characterized by increasing difficulty in recollection, cognition, and performing everyday tasks over time. Recent medical advancements have increased overall life expectancy and have allowed Americans to live longer lives (Beltrán-Sánchez et al., 2015). However, with age being the primary risk factor for dementia, the number of individuals afflicted with AD is set to substantially increase by 2050 (CDC, 2021b). For this reason, it is expected that the cost of AD and other dementias will be over 1 trillion dollars in the United States alone by 2050 (Alzheimer's Association, 2021a). In addition to the economic burden, the psychosocial implications of AD on caregivers and AD patients themselves continues to increase as highlighted by the COVID-19 pandemic. COVID-19 lockdown procedures have severely limited contact with loved ones in care facilities causing both emotional stress and lower perceived well being. In addition, deaths related to AD have increased by 16% during the COVID-19 pandemic (Alzheimer's Association, 2021a). As of now, there is no cure and only limited treatments for AD. Despite decades of research, the disease etiology and pathophysiology remain only partially understood.

1.1.2 Alzheimer's Disease Prevalence and Symptoms

Alzheimer's disease was first identified in 1907 by Alois Alzheimer. It wasn't until the 1960s that Alzheimer's disease was recognized to be the most common form of dementia. Today, the US government spends over 3 billion dollars annually on research of the disease (Alzheimer's Association, 2020b). It is estimated that 6.2 million Americans aged 65 years or older are living with AD. This roughly means that 1 in 9 individuals over the age of 65 are living with AD. The number of people with AD is expected to rise over the next 40 years as the number of older individuals continues to increase as seen in Figure 1 (Alzheimer's Association, 2021a).

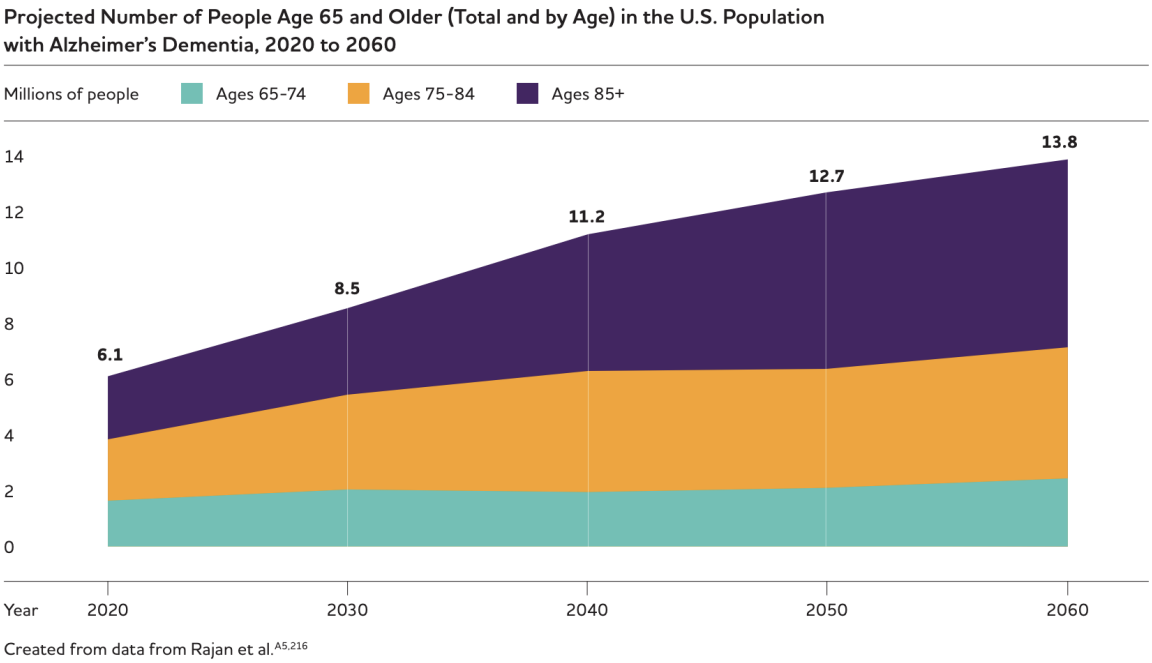

Figure 1. Projected number of people 65+ with AD for the time period 2020-2060 (Alzheimer's Association, 2021a).

Most individuals have late onset of the disease with symptoms starting after the age of 65. Presentation before the age of 65 is considered early onset and has been shown to be more genetically linked than late onset Alzheimer's disease (Alzheimer's Association, 2021b). Duration of the disease is on average 8-10 years, but cases of rapid deterioration have a shorter prognosis (Tang & Gershon, 2003).

Alzheimer's disease is characterized by a decline in cognitive function and memory as well as an increase in negative behavioral symptoms such as apathy, anxiety, and depression (Mielke et al., 2014). Alzheimer's disease is a degenerative brain disease, meaning that its characteristic symptoms develop and worsen overtime. In short, the disease is caused by degeneration of neurons in particular regions in the brain. Normally, the regions controlling memory and cognitive function are affected first. This is exemplified in the early clinical symptoms of difficulty remembering recent events and other's names. These deficits develop throughout the course of the disease to eventually negatively affect other domains such as judgement, behavior and motor control (Alzheimer's Association, 2020a). Progressive loss of cognitive function occurs as the brain becomes more damaged. Normally, patients become fully dependent on their caregivers due to these deficits (Reitz et al., 2011). Unfortunately, it is

hypothesized that changes in the brain actually start up to 20 years before noticeable symptoms (Alzheimer's Association, 2020a).

Studies have found that patients with Alzheimer's disease have a significant impairment in olfaction and perform worse on odor identification tests compared to healthy elderly control subjects (Knupfer & Spiegel, 1986; Tkalčić et al., 2011). It is believed that olfactory dysfunction may be the earliest clinical symptom of AD (Zou et al., 2016). Degenerative damage to the olfactory bulb and olfactory tract at autopsy has been reported (Christen-Zaech et al., 2003; Zou et al., 2016). However, it is still unclear what causes the degeneration of olfactory structures and why it occurs during early in the progression of the disease.

1.1.3 Alzheimer's Disease Etiology and Pathophysiology

Alzheimer's disease is thought to be caused by the development of both extracellular amyloid plaques and intracellular neurofibrillary tangles (Reitz et al., 2011). These changes in the brain along with neuroinflammation and oxidative stress contribute to the symptoms of the disease.

The amyloid cascade hypothesis has long been used to describe the occurrence of amyloid plaques in the Alzheimer's brain and how they lead to disease pathogenesis. According to this model, amyloid precursor protein (APP) is first cleaved by an enzyme called beta-secretase (BACE1). The resulting protein product is then cleaved again by gamma-secretase. These enzymes are part of a larger complex called the presenilin complex (De-Paula et al., 2012). The final peptide formed from this process, amyloid-β_{42} (Aβ42), builds up between neurons and forms harmful amyloid plaques.

The normal role of APP remains unknown, but recent studies suggest it may help with neuron migration in early brain development. When APP is functioning normally, it is cleaved by BACE1 and gamma-secretase enzymes into smaller peptides which are then excreted by neuronal cells. These peptides are either soluble amyloid precursor proteins (sAPP) or amyloid-β peptides of varying lengths. sAPP helps with the formation of neurons throughout development while certain lengths of amyloid-β proteins contribute to brain plasticity (National Institutes of Health, 2020). There are several mutations of the gene encoding APP and the presenilin complex proteins that have been linked to a small percentage of individuals with early onset of Alzheimer's disease.

The basic progression of the disease cascade starts with the accumulation of amyloid-β_{42}. This accumulation results in extracellular amyloid plaque formation which is thought to cause synaptic and neural injury. The injured neurons then continue to be damaged through oxidative injury as their homeostasis mechanisms are altered. This triggers altered cell metabolism resulting in neurofibrillary tangles (NFT). Neurofibrillary tangles are formed by the accumulation of tau protein inside of neural cells. Tau normally plays a role in internal support and stabilization of neurons by assisting microtubules. However, the presence of amyloid plaques promotes the abnormal phosphorylation and aggregation of tau molecules (National Institute on Aging [NIA], 2017). Over time, the resulting neuron dysfunction and death leads to the noticeable symptoms of dementia (Hardy & Selkoe, 2002). The amyloid cascade hypothesis is summarized below as Figure 2.

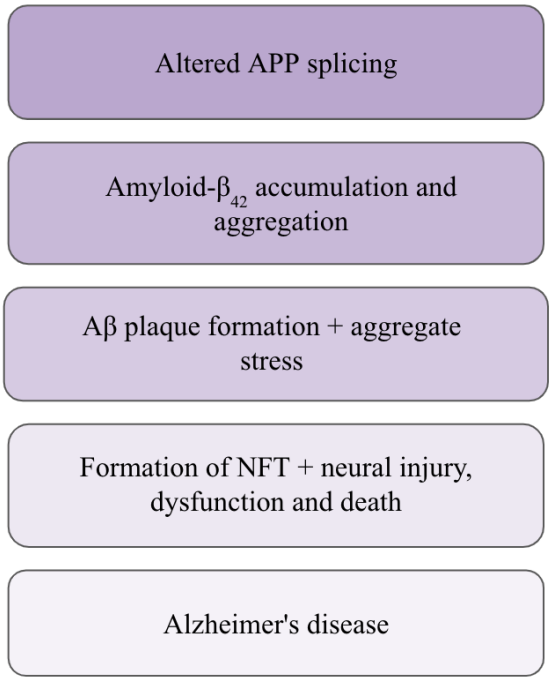

Figure 2. Summary of the amyloid cascade hypothesis.

Recently there has been some dispute over the amyloid cascade hypothesis. The hypothesis has been criticized over its lack of detail. There is research that supports the broad framework of the hypothesis; however, some research has not supported some of the basic components. An example of this is that the number of amyloid plaques in the brain does not correlate well with the degree of cognitive impairment (Hardy & Selkoe, 2002). Although

dispute exists, there have also been a multitude of studies supporting the amyloid cascade hypothesis. For example, mutations in the genes encoding the proteins thought to be involved in plaque formation (APP and presenilin proteins) lead to neurotoxic plaque generation. This has been demonstrated *in vivo* with mouse models. Research has also shown that mutations of proteins involved in plaque clearance and breakdown correlates with an increased risk of developing late-onset AD (Hardy & Selkoe, 2002).

In addition to the development of amyloid plaques, neuroinflammation also has major influences on the progression of AD. Neuroinflammation is mainly due to the body's immune response to the buildup of amyloid plaques and neurofibrillary tangles. Microglia, the resident macrophages of the nervous system, first respond to the presence of abnormal structures in the AD brain. The activation of microglia initiates immune response, such as the release of cytokines, causing chronic inflammation of the area. Over time with perpetual microglial activation, functional and structural damage to neurons occurs (Heneka et al., 2015).

Oxidative stress also has major influences on the progression of AD. Oxidative stress is defined as the imbalance of the production of reactive oxidative species (ROS) and their clearance (antioxidant system). Brain tissue is exposed to oxidative stress through protein oxidation, lipid oxidation, DNA oxidation and glycoxidation due to altered cell metabolism during the progression of AD which may be related to the formation of amyloid plaques (Cheignon et al., 2018; Gella & Durany, 2009). This occurs during the period of aggregate stress. It is hypothesized that oxidative stress also induces and enhances the mediators responsible for neurodegeneration in AD (Huang et al., 2016).

1.1.3 Alzheimer's Disease Risk Factors

There are many biological and environmental risk factors for Alzheimer's disease. It is believed that the interactions between genetic, biological, and environmental risk factors is what ultimately contributes to the development of the disease. In most cases, genetic factors alone are not enough to cause the development of AD.

As previously mentioned, there are several gene mutations that have been correlated with Alzheimer's disease. There are four relatively well known mutations involving the genes encoding the proteins APP, Presenilin 1 (PS1), Presenilin 2 (PS2), and Apolipoprotein E4 (APOE4). The presence of the ε4 allele of Apolipoprotein E (APOE) has been recognized as the

most common genetic risk factor for late onset Alzheimer's disease (Tang & Gershon, 2003). The genetic factors listed above only account for 50% of Alzheimer's disease cases, suggesting that there is still a lot unknown about the genetic factors behind this disease (Tang & Gershon, 2003).

Age is the greatest nonmodifiable risk factor for Alzheimer's disease. Each year past the age of 65, an individual's risk of developing Alzheimer's disease grows. In the 65-74 years old cohort, only 5.3% of individuals have Alzheimer's disease. By 75-84 years old, the percentage of afflicted individuals is 13.8%. In the 85 years or older cohort 34.6% of all individuals have Alzheimer's disease (Alzheimer's Association, 2021a).

Research has shown that there is a sex-bias of Alzheimer's disease with females twice as likely to develop AD than males. This sex-bias is one of the greatest non-modifiable risk factors of Alzheimer's disease. Approximately two thirds of Alzheimer's patients are female (Alzheimer's Association, 2020a). Neurological development is sexually dimorphic meaning men and women have distinct brain morphologies. This sets the stage for different sex based risk factors. For example, women have a greater number of microglial cells in the brain which could contribute to increased neuroinflammation (Podcasy & Epperson, 2016). It is also believed that estrogen may play a role in mediating APOE ε4. However, this neuroprotective interaction between estrogen and APOE ε4 then ceases after menopause. This increases the risk of the development of dementia in older women (Rocca et al., 2014). Women also live longer on average, increasing their age related risk (Podcasy & Epperson, 2016).

There are several identified modifiable risk factors that contribute to the development of Alzheimer's disease. Some of these include cardiovascular disease, traumatic brain injury, type 2 diabetes, body weight, level of education and cognitive engagement (Reitz et al., 2011). As previously stated, researchers believe that it is the interaction of biological and modifiable risk factors that ultimately contributes to the development of the disease. Overall, no single risk factor can explain the onset of AD. Additionally, there may be other risk factors for AD that have not been fully investigated yet.

1.1.4 Current Treatments

There are two classes of AD drugs approved by the FDA: acetylcholinesterase (AChE) inhibitors and N-methyl-d-aspartate (NMDA) receptor antagonists. However, these drugs only

transiently slow the rate of disease development. Most drugs in development aim to modulate the APP processing enzymes, namely inhibiting BACE1 and gamma-secretase enzymes. Others have been designed to promote Aβ clearance (Awasthi et al., 2016). A new drug, Aducanumab, designed to reduce amyloid deposits in the brain recently received accelerated approval this year, however its clinical outcomes remain unknown (NIA, 2021). Aducanumab differs from the other approved drugs in that it is an amyloid beta-directed monoclonal antibody which targets Aβ aggregates (U.S. Food & Drug Administration, 2021). There has been some controversy around the approval because the clinical benefits were only found in a subset of the trial population when the data was re-evaluated (Mullard, 2021).

Research into natural products, such as plant derived compounds, as a possible form of AD treatment has been growing. There are several known natural compounds that originate from plants which have been identified as potential treatments for AD. Some of these include bilobalide sourced from the plant *Ginkgo Biloba*, resveratrol sourced from fruits and nuts, huperzine A sourced from the plant *Huperzia serrata* and punicalagin sourced from pomegranates (Awasthi et al., 2016).

1.2. The Gut Microbiome and the Gut-Brain Axis

The human gut microbiome is composed of over 1,000 different microbial species living in the human gastrointestinal (GI) tract. The microbial cells outnumber the host's cells in a ratio close to 10:1 and contain over 100 times more genes than the number of human genes (Kim & Shin, 2018). The human GI tract is colonized by both strict and facultative anaerobes, or bacteria that do not require oxygen to live. However, facultative anaerobes are found at a much lower frequency. The gut microbiome is dominated by two phyla: the Bacteroidetes and the Firmicutes. The GI tract is first colonized at birth and the gut microbiome develops over time. The composition of the gut microbiome evolves in response to changes in both internal and external factors. Examples of internal factors include physiological factors, intestinal pH, host secretions, drug therapy and immune responses. Examples of external factors include microbial compositions of the local environment, dietary composition, feeding habits and inherited composition of the maternal gut microbiome. The composition of the gut microbiome widely varies between individuals on the bacterial species level because of the unique personal selective pressures established in each GI tract (Bull & Plummer, 2014). Gut microbiome composition

also fluctuates with age and has been found to be sexually dimorphic in recent research (Jašarević et al., 2016).

The gut microbiome has several major involvements in human health and plays a role in human metabolic processes, nutrient absorption, and immune system development. In a healthy model, the gut microbiome produces vitamins, synthesizes amino acids, and helps break down large carbohydrates that the human intestinal cells cannot do on their own. The microbes also help train the immune system, protect the GI tract against pathogenic bacteria through competitive-exclusion and initiate immune responses in the GI tract (Bull & Plummer, 2014). The gut microbes are even responsible for the production, expression, and turnover of certain neurotransmitters such as serotonin and GABA.

Communication between the GI tract and the central nervous system (CNS) occurs along the gut-brain axis (GBA). The gut-brain axis is a bi-directional communication pathway between the gut and the brain that utilizes neural, hormonal, and immunological signaling (Bull & Plummer, 2014). Simply put, this system connects the CNS to the enteric nervous system (ENS) as seen in Figure 3. The brain will communicate with the gut to regulate GI and immune functions. Microbes in the gut can also use this pathway by communicating with intestinal cells that are part of the ENS or directly communicating with the brain through neuroendocrine and metabolic pathways in order to share sensory information about the conditions in the GI tract. Effects on the brain by the microbes in the gut seem to be bacterial strain specific (Carabotti et al., 2015).

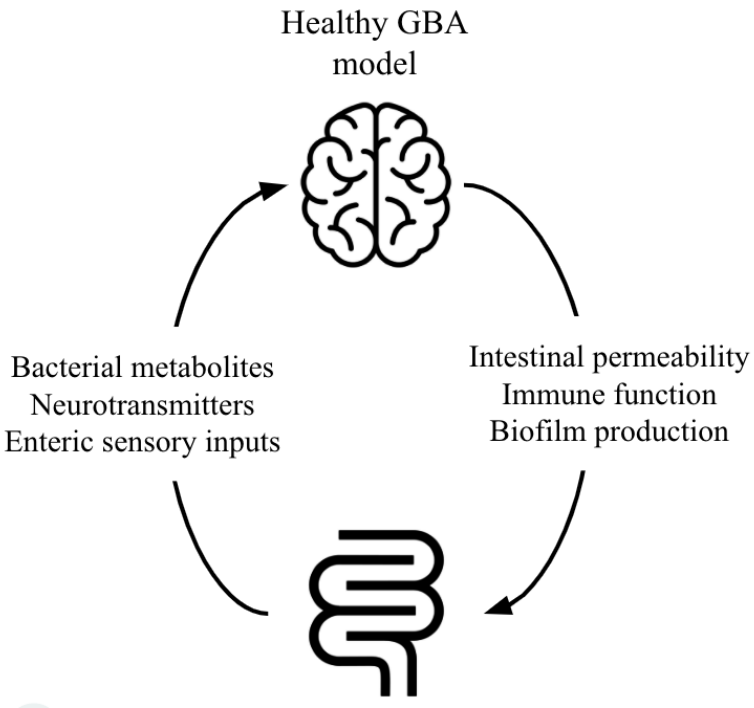

Figure 3. Gut-brain axis communication in a healthy model. The signaling processes are bidirectional, with the brain and gut communicating back and forth to one another.

1.2.1 Gut Microbiome Dysbiosis and Alzheimer's Disease

Dysbiosis, or imbalance, of the gut microbiome has been linked to gut-related diseases such as irritable bowel syndrome and inflammatory bowel disease as well as systemic diseases such as obesity, type 2 diabetes, atopic eczema, and asthma (Bull & Plummer, 2014). Recent research has identified dysbiosis to be associated with several neurological disorders such as anxiety, depression, autism spectrum disorder, Parkinson's disease, and Alzheimer's disease. Generally, dysbiosis disrupts communication in the gut-brain axis and causes breakdown of intestinal permeability, as well as increasing inflammatory responses. Dysregulation of the immune system with age contributes to the gut barrier breakdown. This has been seen to increase proinflammatory cytokines and bacterial endotoxins (ie. lipopolysaccharides) in the bloodstream which in turn causes negative effects on the CNS such as blood-brain barrier impairment and neuro-inflammation (Almeida et al., 2020).

Alteration of the gut microbiome offers another factor to be included in the multi-factor changes required to initiate the amyloid cascade and development of AD. Studies have found that patients with AD have decreased microbial diversity in their gut and the composition of their

gut microbiome is distinctly different from that of age and sex matched controls (Vogt et al., 2017). Research has shown that an altered gut microbiome can contribute to amyloid deposition as well as increase the amount of bacterial metabolites and toxins in the bloodstream, which in turn increases inflammation and neural damage as seen in Figure 4 below (Saji et al., 2020; Vogt et al., 2017).

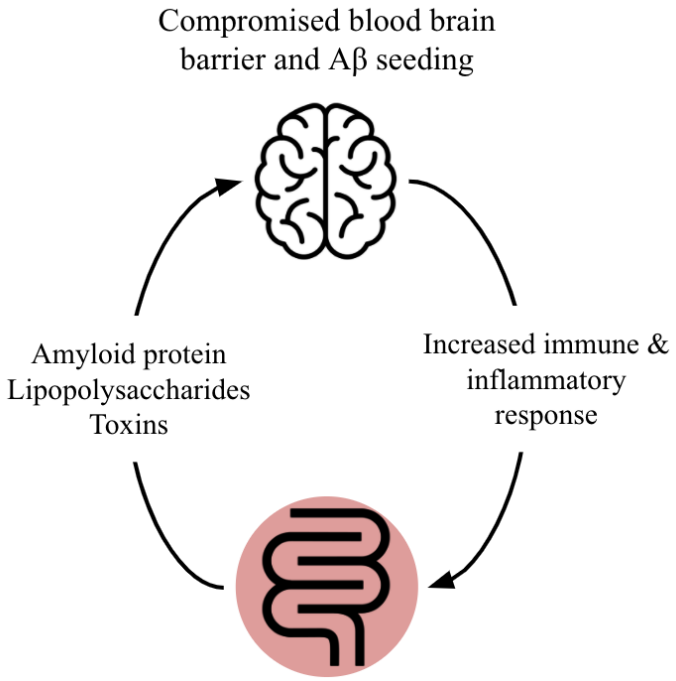

Figure 4. Gut-brain axis communication in a disrupted model with gut microbiome dysbiosis. Increased immune response negatively impacts the composition of the microbes present in the GI tract. Damage to the gut microbiome increases proinflammatory molecules in the bloodstream, which negatively impact the brain.

The microbes in the gut produce amyloids which have similarities to human amyloids in tertiary structure. For example, *Escherichia coli* produce amyloid to help bind to one another and form biofilms. It is postulated that exposure to bacterial amyloids in the gut primes the immune system to later recognize endogenous amyloid proteins in the brain (Kowalski & Mulak, 2019). This immune response causes neurodegeneration as proposed in the amyloid cascade hypothesis. Other research has supported the idea that microbial amyloid promotes the formation of Aβ plaques by acting as a seed for aggregation (Friedland & Chapman, 2017). Bacterial amyloid may cause human amyloid to adopt a different conformation. It has been shown that multiple

bacterial species are capable of amyloid cross-seeding both in vitro and in vivo (Zhou et al., 2012). Bacterial amyloid may also enhance the production of free radicals thereby increasing oxidative stress in the brain (Friedland & Chapman, 2017).

Deterioration of the gut barrier with age and dysbiosis releases harmful bacterial metabolites into the bloodstream. One of these metabolites, lipopolysaccharide (LPS), has been shown to associate with amyloid plaques (Zhan et al., 2018). Lipopolysaccharides are located in the outer membrane of gram negative bacteria and are considered an endotoxin. Blood LPS levels are three times higher in patients with AD when compared to controls (Zhang et al., 2009). LPS levels were also higher in AD brains when compared to aged healthy controls (Zhan et al., 2018). LPS may make its way to the brain after blood brain barrier damage has occurred. Once in the brain, LPS may bind to microglia and cause an inflammatory immune response. In this proposed model, LPS is part of the amyloid cascade, co-localizing and promoting the formation of amyloid plaques (Zhan et al., 2018).

1.3. *C. elegans* as a Model System

Caenorhabditis elegans, or *C. elegans*, is used as a model system to study a variety of topics in biology including developmental biology, neurobiology, and in this case, neurodegeneration (Figure 5). *C. elegans* is a species of free-living nematode originally found in temperate soil environments. These nematodes are small (measuring roughly 1 mm in length as an adult), transparent, progress through a rapid life cycle, and exhibit robust behaviors making them a highly favorable animal model for laboratory applications. They are also easily grown in the lab at low expense and can live on nematode growth agar plates seeded with a bacterial food source, most commonly *Escherichia coli* (Corsi et al., 2015).

Figure 5. Adult wild-type *C. elegans* hermaphrodite (N2 strain).

Wild-type *C. elegans* have a three day life cycle at 20℃ in which they develop from an egg to an egg laying adult (Figure 6). Environmental temperatures will impact *C. elegans* development, causing faster development at higher temperatures and slower development at lower temperatures. On average, they have a lifespan of 2-3 weeks (Corsi et al., 2015).

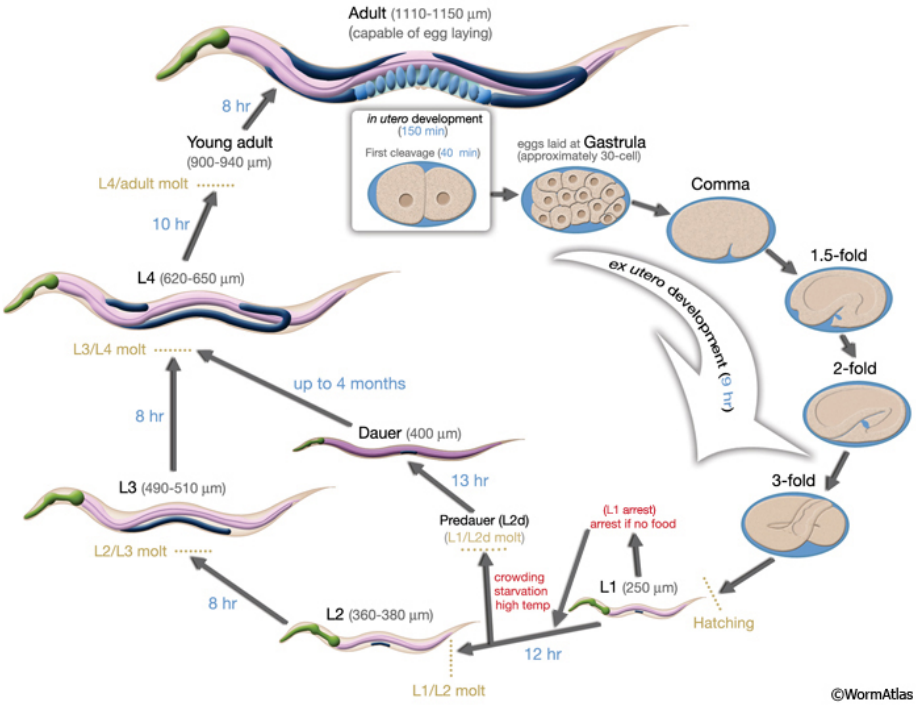

Figure 6. The developmental stages of *C. elegans*. After hatching, *C. elegans* progress through 4 larval stages (L1-L4) to develop into reproducing adults (Altun & Hall, 2009).

Most of the *C. elegans* population is composed of hermaphrodites, although males do exist at a frequency of less than 0.2%. Hermaphrodites carry two X chromosomes (XX), while males only carry a single X chromosome (XO). Both males and hermaphrodites are diploid for the five autosomal chromosomes. Strains with mutations causing a higher incidence of males (him) can be used to increase the number of males in the population. The two sexes of *C. elegans* are not distinguishable until the L4 stage (Corsi et al., 2015).

C. elegans are a useful model for neurobiology research because they have a simple nervous system consisting of only 302 neurons in the adult hermaphrodite and 387 neurons in the adult male compared to the 86 billion neurons in humans (Corsi et al., 2015; Molina-García et al., 2020). The interactions between *C. elegans* neurons have been fully mapped as a neural connectome (Cook et al., 2019). Also, *C. elegans* are an ideal candidate for age related disease research such as neurodegenerative diseases like Parkinson's and Alzheimer's disease because of their rapid life cycle.

C. elegans are also a useful tool in studying potential therapeutics (Chen et al., 2015; Kaletta & Hengartner, 2006; Zheng et al., 2013). *C. elegans* can easily be exposed to treatments through the LB Medium Method of drug delivery in which they consume the treatment as part of the *E. coli* food lawn (Zheng et al., 2013). Compounds can therefore be mixed into the liquid LB media at the appropriate dosage level and delivered to the worms through their food media.

In addition to having several favorable attributes for laboratory use, *C. elegans* also have many molecular similarities to humans making them an ideal model system. As previously mentioned, they are sexually dimorphic which allows them to be an informative model system for sex-bias research. 60-80% of human genes have an ortholog in *C. elegans* and 40% of genes known to cause human disease have an ortholog in *C. elegans* (Corsi et al., 2015). Neurologically, *C. elegans* have many similarities to humans on both a cellular and molecular level.

As previously mentioned, the interactions of *C. elegans* neurons have been fully mapped to the synaptic level. The neural connectome of *C. elegans* is sexually dimorphic, which is also observed in humans (Cook et al., 2019). Most neurons are arranged so that the neuronal cell bodies are located in the head, ventral cord or tail of the worm. Neurons normally have one to two neurites branching from the cell body and are connected to one another through chemical

synapses or gap junctions. *C. elegans* use many of the same neurotransmitters as humans such as dopamine, serotonin, acetylcholine and GABA (Corsi et al., 2015).

Since *C. elegans* are unable to perceive sight and sound, they mainly use olfaction to gain information about environmental conditions as well as to communicate with one another. This sensation and response to environmental chemical stimuli is known as chemoreception. Olfactory signaling is mainly mediated by G protein-coupled receptors which are expressed in olfactory neurons (Corsi et al., 2015).

Responses to chemical stimuli have been well studied and documented. Studies have shown that *C. elegans* have 16 pairs of bilaterally symmetrical chemosensory neurons that respond to a vast array of odorants as seen in Figure 7. Sensory neurons synapse with interneurons (AVA, AVB, AVD, AVE, and PVC) which connect to motor neurons to control locomotion. The chemosensory neurons ASE, AWA, and AWC are known to detect attractants (Hart & Chao, 2010). In contrast, the chemosensory neurons ASH, ADL and AWB are known to detect repellants, with ASH specifically detecting soluble repellants (Hart & Chao, 2010; Sambongi et al., 1999).

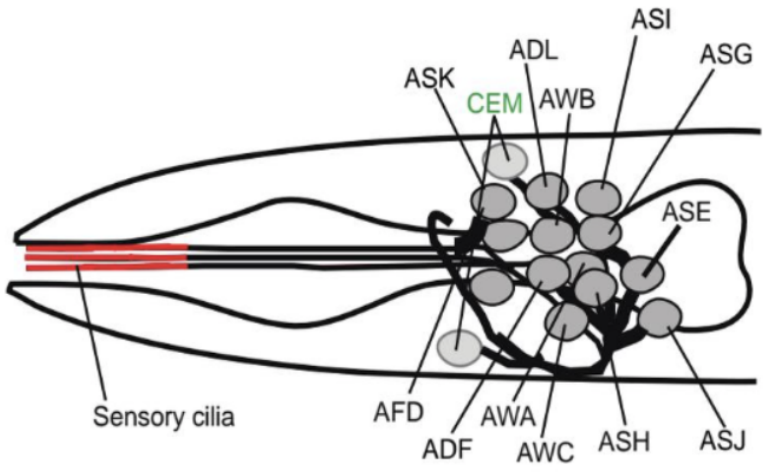

Figure 7. Diagram of *C. elegans* amphid chemosensory neurons (Hart & Chao, 2010).

Due to their well characterized robust behaviors, behavioral assays can be used to study neurobiological changes in *C. elegans*. As previously mentioned, *C. elegans* have strong predictable responses to attractive and aversive stimuli and this can be measured through assays measuring chemoreception (Hart, 2006; Hart & Chao, 2010). In this study the change in

avoidance behaviors to aversive chemical stimuli was used to monitor neurobiological functions. This is discussed in more detail below.

The three aversive chemical stimuli, or repellents, that were used in this study were glycerol, sodium dodecyl sulfate (SDS) and $CuCl_2$. These repeallants were chosen because they have been shown to elicit strong avoidance responses in *C. elegans*. SDS and glycerol are both organic detergents and are sensed by the ASH neuron (Hilliard et al., 2004). $CuCl_2$ contains the heavy metal cation Cu^{2+} and is sensed by the ASH and ADL neurons (Sambongi et al., 1999). Expected behavioral responses to these stimuli have been documented in past studies.

1.3.1 *C. elegans* as a Model for Alzheimer's Disease

It has been demonstrated that *C. elegans* are a powerful tool in studying the molecular and cellular mechanisms of human diseases *in vivo*. Strains with induced mutations using orthologs have been created to model diseases such as Parkinson's disease, amyotrophic lateral sclerosis (ALS), muscular dystrophy, cancers, and more (Markaki & Tavernarakis, 2010). Transgenic mutations also exist to create *C. elegans* strains that model Alzheiemer's disease. As previously discussed, one of the possible mechanisms of the development of AD is the splicing of APP by beta- and gamma-secretases into $A\beta_{42}$ which then aggregates to form harmful amyloid plaques (De-Paula et al., 2012). *C. elegans* have one APP homolog, *apl-1,* located on the X chromosome. This gene is expressed by several cell types and is mainly involved in developmental processes (Markaki & Tavernarakis, 2010).

However, the APP homolog in *C. elegans* does not contain an Aβ domain and *C. elegans* do not have endogenous beta-secretase (BACE). This means that they cannot naturally splice APP into Aβ. In order to model the neurotoxic effects of $A\beta_{42}$ plaques, transgene analysis must be used. A strain created by Dr. Link's lab at the University of Colorado, CL2355, contains a transgene encoding human $A\beta_{1\text{-}42}$. This transgene is under a temperature regulated promoter which provides temporal control over gene expression. Expression of Aβ will only occur once the transgenic worms are exposed to temperatures above 20℃ (Markaki & Tavernarakis, 2010). It should be noted that this strain expresses intraneuronal human $A\beta_{1\text{-}42}$ rather than extracellular plaques (Link, 2005). This transgene also contains a fluorescent marker, allowing for easy identification of individuals with the mutation of interest. This transgenic line has also been shown to have increased levels of reactive oxygen species, as seen in humans (Wu & Luo, 2005).

Similar to humans, *C. elegans* expressing $A\beta_{42}$ pan-neuronally have deficits in olfaction. This deficit in chemoreception was confirmed in a previous MQP which also established techniques to study change in chemosensation in the AD model *C. elegans* strain CL2355. This study demonstrated that the transgenic strain had significantly reduced chemosensation of 0.1% SDS using behavioral assays to measure avoidance (Coyle et al., 2016). The deficit of chemoreception seen in the CL2355 strain was used in this current study as a behavioral marker of Alzheimer's disease related neural damage.

1.3.2 *C. elegans* as a Model for Gut Microbiome Research

Recent research has indicated that *C. elegans* may be an informative model system for gut microbiome studies. Some of the specific attributes of *C. elegans* that make them an ideal system for microbiome research is that they are genetically manipulable, easily decontaminated to make a germ-free model, transparent for fluorescent microbial imaging and have well documented life history readouts that can be used as experimental outcomes. *C. elegans* in the laboratory are normally only exposed to a single strain of *E. coli* as a food source. This means that they have a very limited diversity of microbes in their gut (Zhang et al., 2017). In order to establish the natural diversity of the gut microbiome, three separate studies used 16S rRNA sequencing of samples taken either from wild *C. elegans* or *C. elegans* grown in soil microcosms to characterize the microbes present (Berg et al., 2016; Dirksen et al., 2016; Samuel et al., 2016).

The results of these three studies were used in a meta-analysis to produce what is now considered the full characterization of the *C. elegans* natural gut microbiome. It was found that the natural gut microbiome of *C. elegans* is extremely diverse and holds some consistency across regions. The two dominant microbial families are Gammaproteobacteria and Bacteroidetes (Zhang et al., 2017). Further analysis incorporating two other studies was used to define a model microbiome for use in *C. elegans*. This model microbiome is known as the CeMbio resource (Dirksen et al., 2020).

The CeMbio mix was developed to mimic the *C. elegans* natural food source (Dirksen et al., 2020). The mix includes 12 strains of bacteria that are commonly found in wild *C. elegans* microbiomes as well as in samples from their natural habitats. These strains are listed below in Table 1. All 12 bacterial strains colonize the *C. elegans* gut alone and also as a full community. *C. elegans* adults are colonized by 1,000 - 10,000 bacteria and the bacterial composition of the

gut is distinct from the CeMbio plated lawn. Depending on the conditions, *C. elegans* are colonized by the CeMbio strains in different abundances (Dirksen et al., 2020).

Table 1. The 12 CeMbio strains used in the CeMbio inoculum (Dirksen et al., 2020).

Strain name	Strain Taxonomy
CEenent1	*Enterobacter hormaechei*
BIGb0170	*Sphingobacterium multivorum*
BIGb0172	*Comamonas piscis*
BIGb0393	*Pantoea nemavictus*
MSPm1	*Pseudomonas berkeleyensis*
MYb10	*Acinetobacter guillouiae*
MYb11	*Pseudomonas lurida*
MYb71	*Ochrobactrum vermis*
JUb19	*Stenotrophomonas indicatrix*
JUb44	*Chryseobacterium scophthalmum*
JUb66	*Lelliottia amnigena*
JUb134	*Sphingomonas molluscorum*

It was also found that the CeMbio strains influenced *C. elegans* biology. *C. elegans* growth rates were increased when fed the CeMbio strains as a community. When modeling the metabolic network of the 12 bacterial strains, it was found that the CeMbio strains may provide *C. elegans* with metabolites important for growth (Dirksen et al., 2020). Even in non-disease states, a natural composition of the gut microbiome had huge implications on *C. elegans* health. Overall, use of the CeMbio resource provides *C. elegans* with a more ecologically relevant microbiome that can be used to better understand the relationships between microbes and their host (Dirksen et al., 2020).

1.4 Punicalagin as Treatment

Punicalagin is a polyphenol found in pomegranates. It has antioxidant properties, meaning it neutralizes free radicals and reduces oxidative stress. As an antioxidant, punicalagin has the potential of reducing some of the oxidative stress seen in AD due to changes in cell metabolism by binding to ROS and preventing them from causing damage. Additionally, research has shown that punicalagin reduces LPS induced oxidative stress and neuroinflammation (Kim et al., 2017; Olajide et al., 2014). One of these studies also showed that punicalagin reduces LPS induced amyloid plaque formation (Kim et al., 2017).

In *C. elegans*, punicalagin has been shown to have health promoting effects. For example, one study showed that pomegranate juice extract increased the life span and reduced intestinal fat deposition in *C. elegans*. A past MQP by Coyle et al. found that treatment with punicalagin was able to mediate chemoreceptor deficiencies seen in the *C. elegans* AD model strain, CL2355. With this knowledge, this current study aimed to validate the observed rescue by punicalagin and to also extend the research by using new aversive cues when testing for chemoreception rescue after punicalagin treatment.

1.5 Project Overview

This project first aimed to establish the baseline chemoreception of the *C. elegans* AD model strain CL2355 using three aversive stimuli: 0.1% SDS, 10mM $CuCl_2$ and 1M glycerol. This was done to assess whether the CL2355 strain exhibited a total loss of chemoreception with induction of Aβ plaques, or if the strain retained some sensitivity to aversive stimuli. This project then aimed to investigate the therapeutic effects of gut microbiome supplementation with CeMbio strains and treatment with punicalagin extract by observing changes in chemoreception with treatment. Avoidance assays were used to measure chemoreception to aversive stimuli throughout the experiment.

2.0 Methodology

2.1 Worm Strains and Maintenance

N2 (wildtype), *him-5 (CB4088 (him-5(e1490))*, CL2122 (*smg-1*ts; *dvIs15* [(pPD30.38) *unc-54*(vector) + (pCL26) *mtl-2*::GFP]), and CL2355 (*smg-1*(cc546); pCL45 [P*snb-1*::human Amyloid beta 1-42::3' UTR (long); P*mtl-2*::GFP]) strains were obtained through the Caenorhabditis Genetics Center (CGC).

C. elegans strains were maintained on 60 mm nematode growth media (NGM) plates seeded with the corresponding bacterial media of their experimental group as a food source (NGM: 3g/L NaCl, 2.5g/L peptone, 17g/L agar, 25mM KPO_4 buffer [pH = 7], 1mM $MgSO_4$, 1mM $CaCl_2$, 0.0129mM cholesterol in ethanol, H_2O to volume). Plates were seeded with their designated food source using either a micropipette or a serological pipette. Seeded lawns were allowed to dry before moving worms onto the plates. Stock strains were maintained on plates seeded with OP50 *E. coli* in LB media (LB: 10g/L NaCl, 10g/L tryptone, 5g/L yeast, H_2O to volume). Microbiome supplementation groups were maintained on plates seeded with 100uL of CeMbio bacterial mix at an OD of 1 in PBS (see section 2.3.1). Punicalagin treatment groups were maintained on plates seeded with 100uL of OP50 *E. coli* + punicalagin extract at 1.2 x 10^{-7} M in LB media (see section 2.3.2).

Worms were passed onto new seeded plates every 2-3 days by pick transfer to prevent starvation. A worm pick was used for pick transfers and was made by fusing a flattened platinum wire to the end of a 5mL glass Pasteur pipette. The pick was flame sterilized between each worm transfer. N2 and *him-5* strains were maintained at 20℃. CL2355 and CL2122 strains were maintained at 16℃ because of their temperature sensitive transgenes.

2.2 Heat Shock Protocols

2.2.1 Heat Shock for Baseline Chemoreception Experiments

The heat shock protocol was used to induce expression of pan-neuronal amyloid beta in the CL2355 strain. The CL2122 strain was also heat shocked as a control for the CL2355 strain. First, eggs were obtained through bleaching protocol. Two drops of 30uL worm bleach were placed on far ends of an unseeded plate. Then five gravid worms of the desired strain were

picked into each of the bleach spots causing the worms to lyse open and release eggs. This bleach plate was allowed to dry at 20℃ overnight. After drying, the L1s on the plate were washed off the plate and into a 1.5mL centrifuge tube using 1mL of M9. The worms were then washed by mixing them in the M9 before allowing them to settle to the bottom of the tube by gravity and then aspirating the M9 from top. This was repeated three times. Once washed, the excess M9 was removed so about 100uL remained. The worms were then mixed thoroughly in the 100uL and 25uL of this mixture was added to 3-4 previously seeded plates with OP50. These plates were then placed in a 25℃ incubator to heat shock for 48 hours. After 48 hours, the heat shock plates were removed from the 25°C incubator and were allowed to rest for one hour at room temperature. After rest, the worms were then used in avoidance assays.

2.2.2 Heat Shock for Treatment Experiments

Due to contamination issues, a new heat shock protocol was developed and followed for the remainder of the experiment. For both strains, 4 L4 stage worms were picked onto a plate seeded with the corresponding bacterial media of their experimental group as a food source (either OP50, CeMbio, or OP50 + punicalagin). The worms were allowed to lay eggs for 48 hours at 16℃. After 48 hours, the now adult worms were removed from the plate and the resulting plate with eggs and L1 stage larvae was placed in a 25℃ incubator to heat shock for 48 hours. After 48 hours, the heat shock plates were removed from the 25℃ incubator and were allowed to rest for one hour at room temperature. After rest, the worms were then used in avoidance assays.

2.3 Treatments

2.3.1 CeMbio Mix

All 12 CeMbio bacterial strains were obtained through the CGC on LB plates. To create the CeMbio mix, strains were first grown up separately in 10 mL of liquid LB for 48 hours at 25℃. After growth, strains were spun down by centrifugation for 10 minutes at 4℃ and 3900 rpm. The resulting supernatant was poured off and sample pellets were resuspended in 600 uL of PBS (7.31g/L NaCl, 2.36g/L Na_2HPO_4, 1.31g/L NaH_2PO_4•$2H_20$, H_2O to volume, pH = 7.0-7.2). Samples were diluted 1:10 by taking 100 uL of each sample and adding it to 900 uL of PBS in a cuvette. The optical density (OD) of each diluted sample at 600 nm was found using a Multiskan

Spectrum spectrophotometer. Each sample was then diluted down to an OD of 1 in PBS. Samples were mixed together in equal volume to result in a CeMbio mix with an OD of 1. The final CeMbio mix was then used to seed plates (100uL per plate) for gut microbiome supplementation experiments. The CeMbio mix was remade on a weekly basis. The 12 stock CeMbio strains were restreaked from previously frozen 1:1 glycerol stocks stored at -80℃ onto fresh LB plates every three months.

2.3.2 Punicalagin

Punicalagin for treatment was made following previous protocols found in Consedine et al. and Coyle et al. (Consedine et al., 2018; Coyle et al., 2016). A punicalagin extract mixture was first made up by diluting a 40% punicalagin stock in MilliQ water to reach a final concentration of 1.2 x 10^{-6} M. This solution was then filtered using a 0.22-micron filter under a hood to reduce the risk of contamination. Once the solution was made at 1.2 x 10^{-6} M, 10mL was added to 90mL of LB media then inoculated with OP50 to create a OP50 + punicalagin mixture at 1.2 x 10^{-7} M. This OP50 + punicalagin mix was then used to seed plates (100uL per plate) for the punicalagin treatment experiments. The mixture was used for a month and was stored at 4℃ in between uses.

2.4 Avoidance Assay

Avoidance assays were used to observe chemoreception abilities of N2, CL2122 and CL2355 strains under different conditions. Unseeded NGM plates were used as assay plates. These unseeded NGM plates were first allowed to dry for 30 min to 1 hour depending on the humidity of the room. The plates were given more time to dry on days with higher humidity (>40%). Once dry, 10 adult worms were added to each assay plate by pick transfer. Worms were then given 5-10 minutes to acclimate to the new plate. After set-up, the worms were tested using the drop assay protocol found in Worm Book and originally described in work done by Hilliard, Bargmann, and Bazzicalupo (Hillard et al., 2002). Assays were only completed in conditions of <40% humidity and <25℃.

Drops were delivered to each worm using a mouth pipette fitted with a fine micro needle tip made by pulling a 10uL glass capillary tube over a flame. All 10 worms were first tested with a solvent control by dropping a roughly 5 nL drop of liquid behind the tail of a forward moving

worm so it would be wicked up to the nose by capillary action. After testing avoidance to the solvent control, plates were given 5 minutes to dry. The drop protocol was then repeated, but this time using an aversive chemical cue. Avoidance was quantified by observing the worm's behavior in response to the drop within 4 seconds. If the worm reversed direction over two body bends or made a 90° turn from its original direction, it was documented as having avoidance to the stimulus. Examples of non-avoidance and avoidance behavior is shown in Figure 8.

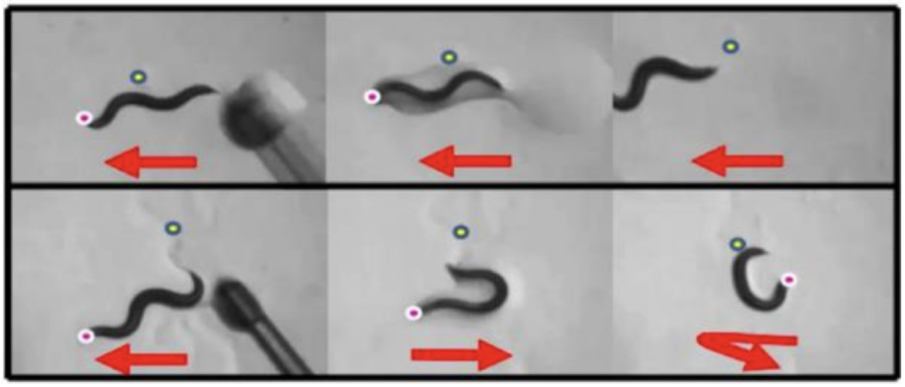

Figure 8. Non-avoidance vs. avoidance behavior of *C. elegans* in response to a drop of a chemical cue. The red arrow marks the direction of forward motion. The top row shows a worm exhibiting non-avoidance behavior by continuing to move forward after the drop is delivered. The bottom row shows a worm exhibiting avoidance behavior by turning around after the drop is delivered (Chute, 2018).

Avoidance index was then calculated for each assay plate by dividing the number of worms with avoidance by the number of worms tested following the equation presented below as Equation 1. In most cases, at least 10 assay plates were tested for each condition. Four different aversive chemicals were used throughout testing: 0.1% sodium dodecyl sulfate (SDS), 1M glycerol and 10mM $CuCl_2$. Concentrations of the repellants were chosen based on those used in literature (Hilliard et al., 2002; Hilliard et al., 2004; Sambongi et al., 1999). Both the SDS solution and the glycerol solution were made up in M9 buffer (M9: 3g/L KH_2PO_4, 6g/L Na_2HPO_4•$2H_2O$, 5g/L NaCl, 1mL 1M $MgSO_4$, 1L H_2O) while the $CuCl_2$ solution was made up in M13 buffer (M13: 3mL 1M Tris, 2mL 5M NaCl, 1mL 1M KCl, 94mL H_2O). The corresponding buffer for each adverse chemical was used as the respective solvent control (SC) in testing.

$$Avoidance\ Index = \frac{Number\ of\ worms\ with\ avoidance}{Number\ of\ worms\ tested} \qquad (1)$$

3.0 Results and Discussion

3.1 Alzheimer's Disease Model Baseline Chemoreception

Three repellants were selected to study the chemoreception loss of the AD model *C. elegans* strain, CL2355. Avoidance assays were used to test each of the three repellants: 0.1% SDS, 10mM $CuCl_2$, and 1M glycerol. In each assay, the control strains used were wildtype N2 and AD model control CL2122. N2 strains were grown at 20°C, while CL2122 and CL2355 strains were previously heat shocked at 25°C for 48 hours. Overall, it was found that the CL2355 strain retained some level of sensitivity to different aversive stimuli rather than experiencing a universal loss of chemoreception. However, this level of sensitivity was diminished compared to controls.

3.1.1 Avoidance Assays with 0.1% SDS

Avoidance to 0.1% SDS was tested in N2, CL2122 and CL2355 strains and the results are shown in Figure 9. The average avoidance index of wildtype N2 was 0.65 ± 0.0915. This avoidance index is consistent with data found in literature (Hilliard et al., 2002). The average avoidance index of the AD model control CL2122 was 0.53 ± 0.0884. The average avoidance index of the AD model CL2355 was 0.44 ± 0.0842. This avoidance index for CL2355 was similar to that found in Coyle et al. (Coyle et al., 2016).

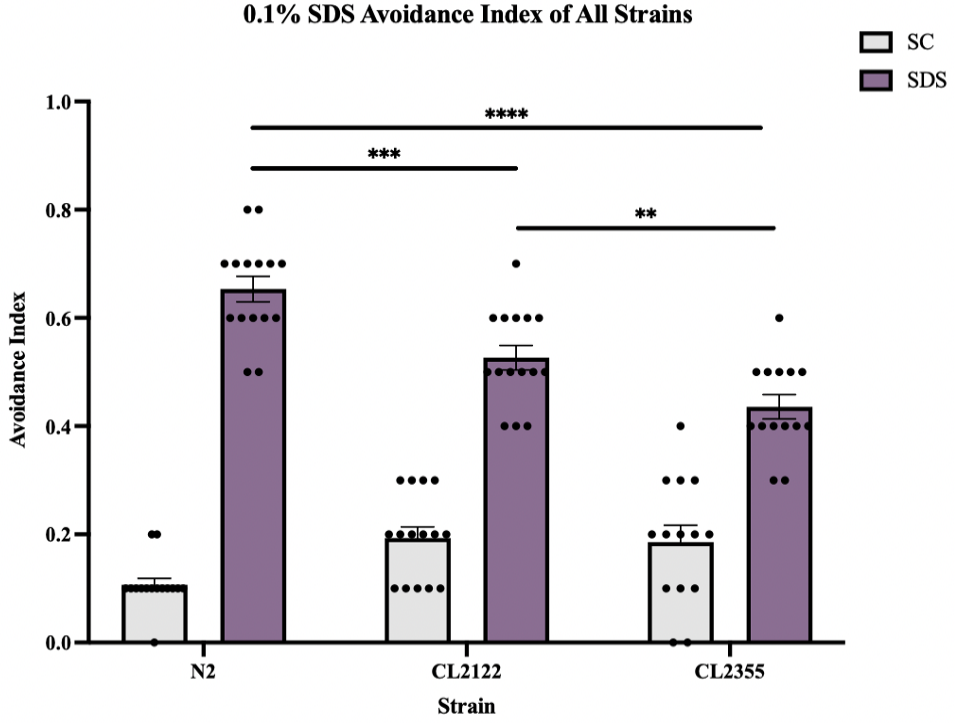

Figure 9. Average avoidance index of all strains to 0.1% SDS. SC = Solvent control. Error bars are SEM. n = 15. Welch's t-test. ** $p < 0.01$, ***$p < 0.001$, ****$p < 0.0001$.

Overall, the AD model CL2355 had a significantly lower avoidance index compared to the avoidance index of its control, CL2122. This means that CL2355 had deficient avoidance to 0.1% SDS. This can be further interpreted as having a deficiency in the chemoreception of 0.1% SDS. The CL2122 control strain had a significantly lower avoidance index when compared to wildtype N2. The difference in the behavior of CL2122 and N2 may be attributed to the heat shock protocol completed for CL2122. Completing this heat shock protocol makes CL2122 a more appropriate control for CL2355.

The significant difference in avoidance of CL2355 compared to its control CL2122, supports the conclusion that CL2355 is deficient in chemoreception of 0.1% SDS. This agrees with data from a past MQP which found CL2355 to be deficient in sensation of and response to 0.1% SDS (Coyle et al., 2016). Deficiency in the chemoreception of 0.1% SDS indicates Aβ plaque interference with olfaction processes. This may be due to the physical presence of the plaques themselves, or a downstream effect of these plaques such as neuroinflammation or oxidative stress. It is also possible that the aversive cue is being sensed by the corresponding

primary sensory neuron, but neural damage downstream prohibits an avoidance response to the cue. In either case, the expression of Aβ plaques results in the disruption of normal olfactory function.

3.1.2 Avoidance Assays with 10mM $CuCl_2$

Avoidance to 10mM $CuCl_2$ was tested in N2, CL2122 and CL2355 strains and the results are shown in Figure 10. The average avoidance index of wildtype N2 was 0.65 ± 0.0874. This avoidance index is consistent with data found in literature (Sambongi et al., 1999). The average avoidance index of the AD model control CL2122 was 0.73 ± 0.103. The average avoidance index of the AD model CL2355 was 0.37 ± 0.0799.

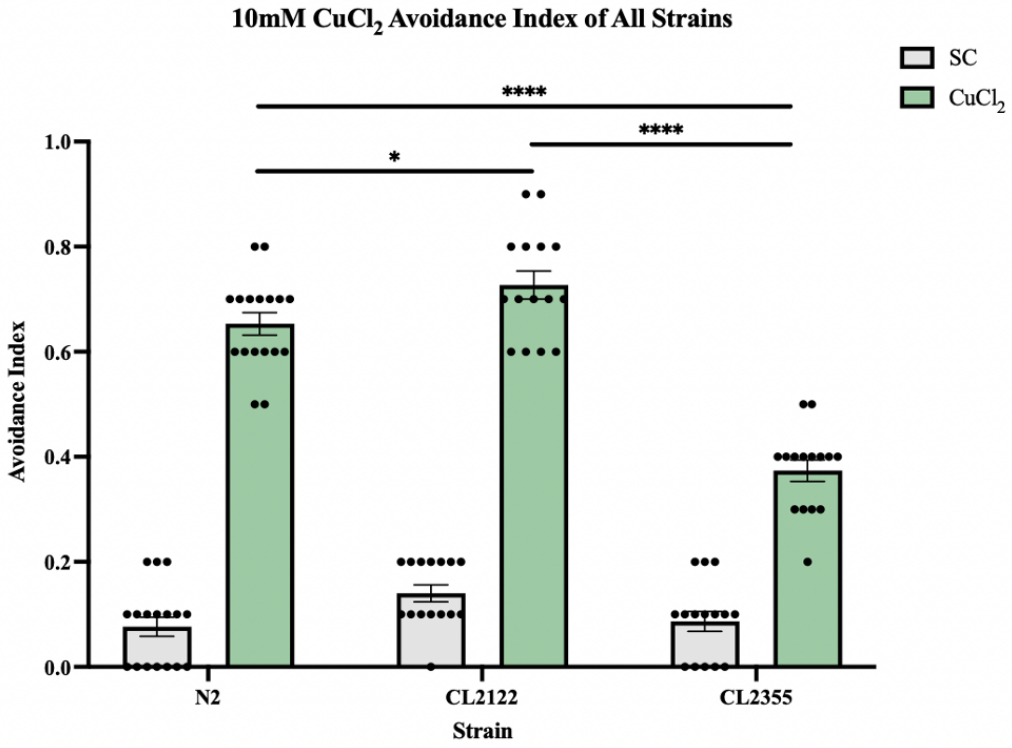

Figure 10. Average avoidance index of all strains to 10mM $CuCl_2$. SC = Solvent control. Error bars are SEM. n ≥ 15. Welch's t-test. * $p < 0.05$, ****$p < 0.0001$.

Overall, the AD model CL2355 had a significantly lower avoidance index compared to the avoidance index of CL2122. This means that CL2355 had decreased avoidance to 10mM $CuCl_2$. This can be further interpreted as having a deficiency in the chemoreception of 10mM

$CuCl_2$. It should be noted that the CL2122 control strain had a significantly higher avoidance index when compared to N2. Again, the difference in the behavior of CL2122 and N2 may be attributed to the heat shock protocol completed for CL2122.

The significantly lower avoidance index and therefore deficient chemoreception of 10mM $CuCl_2$ by CL2355 further indicates that Aβ plaques are interfering with olfaction processes. Again, this may be due to the physical presence of the plaques themselves, or a downstream effect of plaque formation.

3.1.3 Avoidance Assays with 1M glycerol

Avoidance to 1M glycerol was tested in N2, CL2122 and CL2355 strains and the results are shown in Figure 11. The average avoidance index of wildtype N2 was 0.64 ± 0.0853. The average avoidance index of the AD model control CL2122 was 0.59 ± 0.0829. The average avoidance index of the AD model CL2355 was 0.63 ± 0.0826.

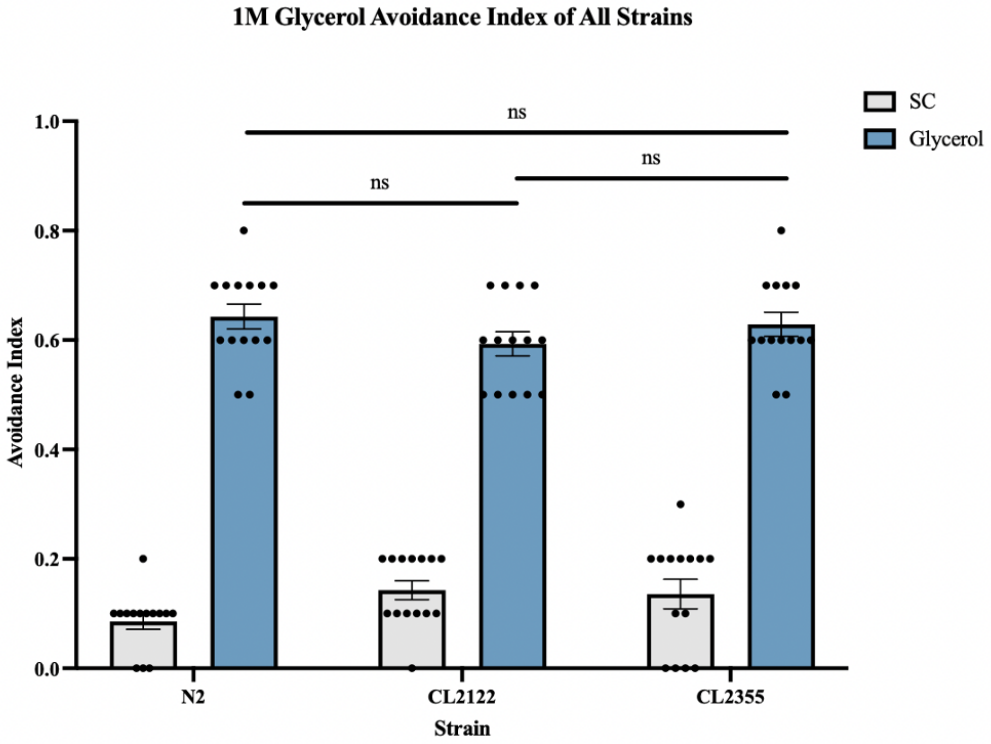

Figure 11. Average avoidance index of all strains to 1M glycerol. SC = Solvent control. Error bars are SEM. n = 15. Welch's t-test. "ns" = not significant

Overall, there was no significant difference in the average avoidance index between the

wildtype, AD control and AD model strains as seen in Figure 11. All 3 strains displayed similar avoidance behavior to 1M glycerol. Since there was no significant difference between the avoidance indices of CL2355 and its control CL2122, it can be interpreted that the AD model CL2355 retains chemoreceptor sensitivity to the aversive stimulus of glycerol at 1M. Furthermore, the data supports the conclusion that the AD model does not experience a universal loss of chemoreception. It instead retains some sensitivity to aversive stimuli.

It is possible that the AD model retained some sensitivity to aversive stimuli and that this sensitivity is diminished compared to controls. Instead of only being sensitive to certain stimuli, the AD model is sensitive to all stimuli but needs a much higher stimulus to elicit the same response. In other words, the formation of Aβ plaques could have caused neural damage that resulted in sensitivity decrease, not full olfactory loss. The aversive stimulus of 1M glycerol may have been much stronger than 0.1% SDS and 10mM $CuCl_2$ and this is why it still stimulated an avoidance response. In this explanation, the decrease in sensitivity of aversive stimuli by Aβ plaque formation means that chemoreception is stimuli concentration or dose dependent.

Alternatively, the three stimuli could be sensed through different pathways and Aβ plaque formation did not interfere with the pathway responsible for glycerol sensation. This allowed the worms to retain chemoreception to 1M glycerol but lose chemoreception to SDS and $CuCl_2$. However, all three stimuli are sensed by the ASH neuron. This means that if differences were present, they would have to be further downstream. Additionally, further testing indicated that CL2355 retains sensitivity to SDS at higher concentrations (Supplementary Figure 5; Appendix C). This supports the dose dependent explanation rather than the differences in neural pathway interference explanation.

3.2 Avoidance to Aversive Stimuli After Gut Microbiome Supplementation

After the baseline chemoreception of the AD model was established, gut microbiome supplementation was used to try to improve chemoreception of both 0.1% SDS and 10mM $CuCl_2$. All three *C. elegans* strains (N2, CL2122 and CL2355) were fed CeMbio bacterial strains from hatching to the time of assay as a form of gut microbiome supplementation. CL2122 and CL2355 strains were heat shocked on plates seeded with CeMbio strains. The repellant of 1M glycerol was not chosen for treatment studies because CL2355 did not show a loss of chemoreception to this chemical.

3.2.1 Avoidance Assays with 0.1% SDS After Gut Microbiome Supplementation

Avoidance assays were completed to evaluate the impact of microbiome supplementation with CeMbio strains on chemoreception of 0.1% SDS. The average avoidance index of the AD model control CL2122 after treatment was 0.58 ± 0.0837. The average avoidance index of the AD model CL2355 after treatment was 0.46 ± 0.103. Figure 12 shows a comparison of both treatment strains to their baseline avoidance indices. A Welch and Brown-Forsythe ANOVA test was run between treatment and non-treatment solvent controls and found no significant difference. For this reason, solvent control data have been omitted from Figure 12 and can be found in Supplementary Figure 1 (Appendix C).

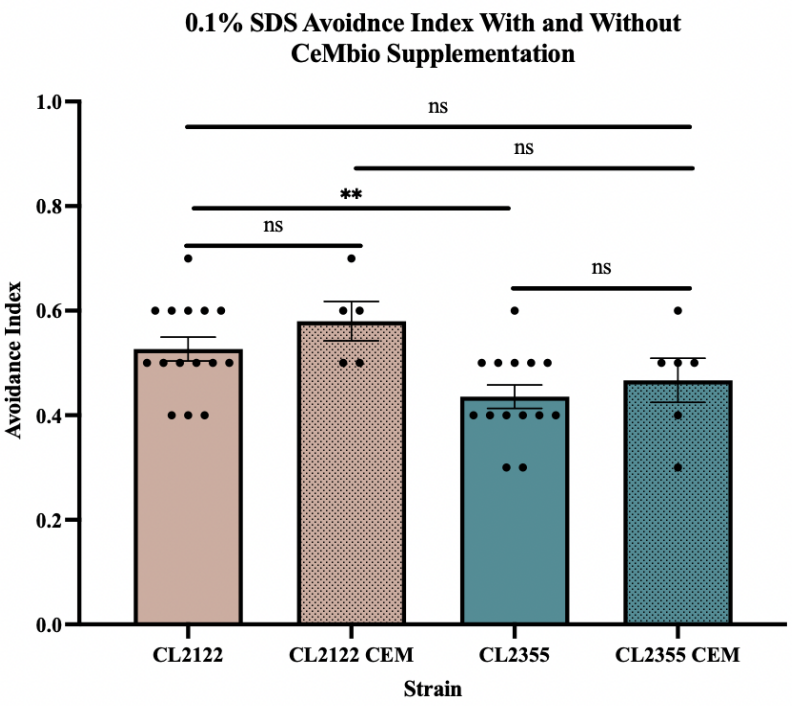

Figure 12. Average avoidance index to 0.1% SDS with and without gut microbiome supplementation with CeMbio strains (CEM). SC = Solvent control. Error bars are SEM. n ≥ 5. Welch's t-test. “ns” = not significant, **p < 0.01.

Overall, the data show a partial increase of avoidance behavior. There was no significant difference in avoidance to 0.1% SDS when comparing the untreated and treated CL2122 and CL2355 strains. As seen before in Figure 9, there is a significant difference between untreated CL2122 and untreated CL2355 strains. Although there is no significant difference between the

untreated and treated CL2355 strains, there is an indication that the microbiome supplementation may be partially increasing avoidance response. There was no significant difference in avoidance to 0.1% SDS when comparing the treated CL2355 strain to the control strain, CL2122. This means that the treated CL2355 strain exhibited avoidance behavior similar to that of the control. If microbiome supplementation were a successful therapeutic, the treated CL2355 strain would have significantly different avoidance than the untreated CL2355 strain. However, since the treated CL2355 is not significantly different from the control worms, the data support a partial improvement of chemoreception. Overall, this can be interpreted as gut microbiome supplementation having some therapeutic impact on avoidance behavior to 0.1% SDS and therefore chemoreception of 0.1% SDS.

3.2.2 Avoidance Assays with 10mM $CuCl_2$ After Gut Microbiome Supplementation

Avoidance assays were completed to evaluate the impact of microbiome supplementation with CeMbio strains on chemoreception of 10mM $CuCl_2$. The average avoidance index of the AD model control CL2122 after treatment was 0.79 ± 0.134. The average avoidance index of the AD model CL2355 after treatment was 0.49 ± 0.0835. Figure 13 shows a comparison of both treatment strains to their baseline avoidance indices. A Welch and Brown-Forsythe ANOVA test was run between treatment and non-treatment solvent controls and found no significant difference. For this reason, solvent control data has been omitted from Figure 13 and can be found in Supplementary Figure 2 (Appendix C).

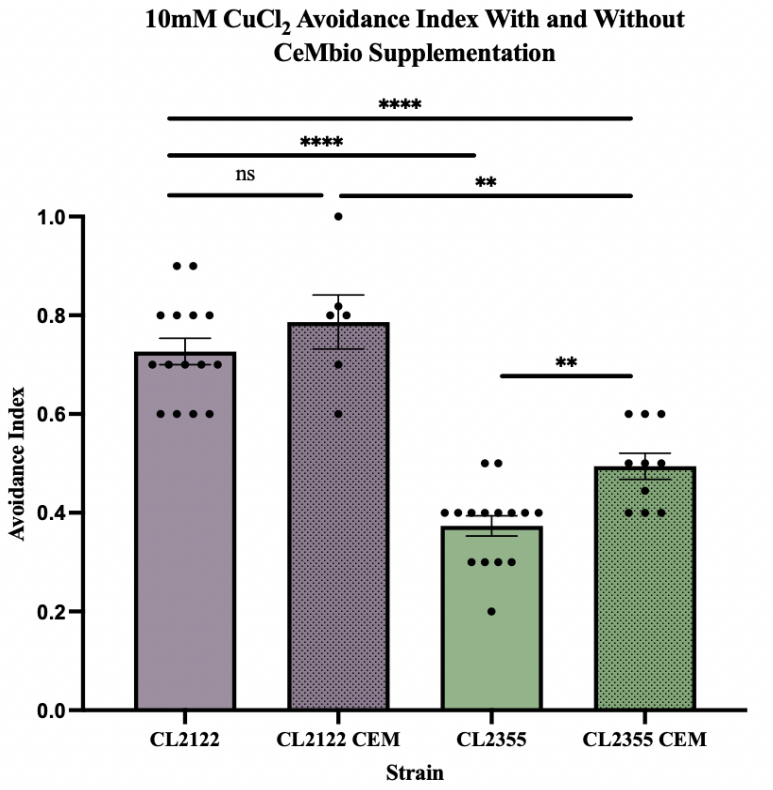

Figure 13. Average avoidance index to 10mM $CuCl_2$ with and without gut microbiome supplementation with CeMbio strains (CEM). SC = Solvent control. Error bars are SEM. $n \geq 6$. Welch's t-test. "ns" = not significant, **$p < 0.01$, ****$p < 0.0001$.

There was a significant increase in avoidance to 10mM $CuCl_2$ when comparing untreated and treated CL2355 strains. However, there was still a significant difference between the treated CL2355 strain and both untreated and treated CL2122 controls. The treated CL2355 strain had a significantly lower avoidance index than the controls. If microbiome supplementation were a successful therapeutic, the avoidance index of the treated CL2355 strain would not be significantly different from the controls but would be significantly different than the untreated CL2355 strain. Since the results only agree with the second part of this statement, the data support a partial improvement of avoidance behavior to 10mM $CuCl_2$ after gut microbiome supplementation. Therefore, gut microbiome supplementation has some therapeutic impact on avoidance behavior to 10mM $CuCl_2$ and therefore chemoreception of 10mM $CuCl_2$.

Gut microbiome supplementation may have partially improved the chemoreception sensitivity of the treated CL2355 strain compared to its untreated baseline. This would mean that

the treatment did not fully restore chemoreception sensitivity of 0.1% SDS or 10mM $CuCl_2$. This is why avoidance to both of these cues increased, but not to levels that would indicate a full therapeutic benefit. If the sensitivity of CL2355 chemoreception were increased to the same level as seen in controls, then it would have been considered a successful intervention either preventing or rescuing chemoreception.

Overall, it can be interpreted that gut microbiome supplementation had a positive impact on the defective chemoreception of CL2355 but was unable to fully reverse the deficit. This was seen in the partially improved chemoreception of both 0.1% SDS and 10mM $CuCl_2$. Although the *C. elegans* were exposed to and ingested all 12 strains of their natural microbiota, there was no confirmation that the 12 strains colonized their gut. If the AD model *C. elegans* did have disrupted gut microbiota, gut microbiome supplementation with healthy strains would help reconstitute the gut but may not fully recolonize the gut to healthy composition. The partial reconstitution may have translated to the partial increase of avoidance behavior.

Supplementation of the gut microbiome may have increased the number of anti-inflammatory microbes thereby preventing damage or further damage to the gut barrier. Restoring the health of the gut barrier would decrease the amount of harmful bacterial metabolites and toxins in blood circulation, both of which are known to cause neural damage. This would decrease levels of oxidative stress and neuroinflammation. However, it is unclear in this case if the supplementation would have neuroprotective versus restorative effects because the worms were treated throughout their life span.

3.3 Avoidance to Aversive Stimuli After Punicalagin Treatment

Treatment with punicalagin extract was used to try to improve chemoreception of both 0.1% SDS and 10mM $CuCl_2$. All three *C. elegans* strains (N2, CL2122 and CL2355) were fed OP50 + punicalagin from hatching to the time of assay as a form of punicalagin treatment. CL2122 and CL2355 strains were heat shocked on plates seeded with OP50 + punicalagin. Again, the repellant of 1M glycerol was not chosen for recovery studies because CL2355 did not show a loss of chemoreception to this chemical during baseline testing.

3.3.1 Avoidance Assays with 0.1% SDS After Punicalagin Treatment

Avoidance assays were completed to evaluate the impact of punicalagin treatment on

chemoreception of 0.1% SDS. The average avoidance index of the AD model control CL2122 after treatment was 0.56 ± 0.0978. The average avoidance index of the AD model CL2355 after treatment was 0.57 ± 0.148. Figure 14 shows a comparison of both treatment strains to their baseline avoidance indices. A Welch and Brown-Forsythe ANOVA test was run between treatment and non-treatment solvent controls and found no significant difference. For this reason, solvent control data has been omitted from Figure 14 and can be found in Supplementary Figure 3 (Appendix C).

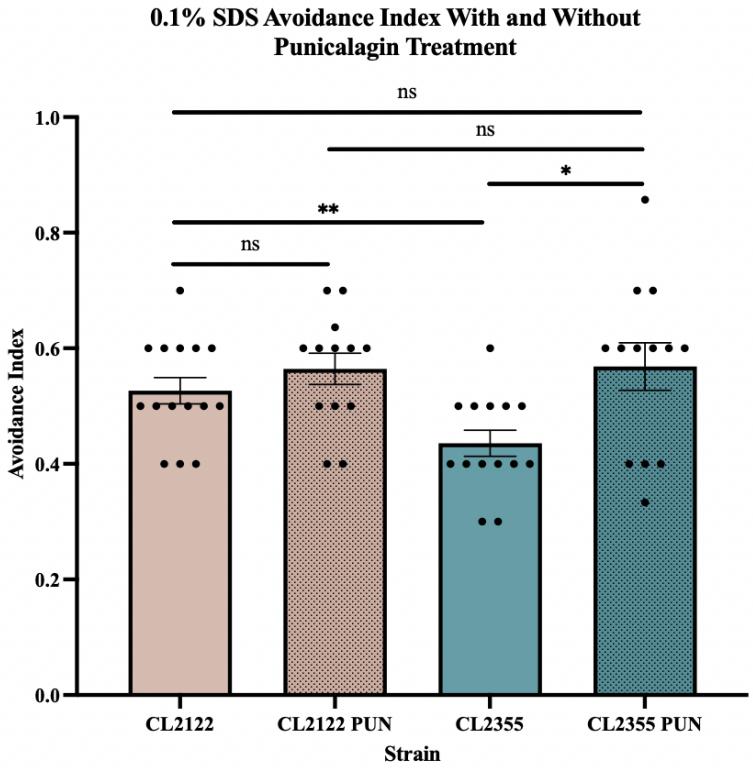

Figure 14. Average avoidance index to 0.1% SDS with and without punicalagin treatment (PUN). SC = Solvent control. Error bars are SEM. n ≥ 13. Welch's t-test. “ns” = not significant, *p < 0.05, **p < 0.01.

There was a significant increase in avoidance to 0.1% SDS when comparing treated to untreated CL2355 strains. Additionally, there was no significant difference in avoidance to 0.1% SDS when comparing treated CL2355 to both untreated and treated CL2122 control strains. The treated CL2355 strain did not act significantly different from the controls but did act significantly

different than the untreated CL2355 strain. This indicates a full therapeutic effect. The data support that punicalagin treatment improves the deficit in avoidance behavior to 0.1% SDS. This finding is consistent with a previous MQP (Coyle et al., 2016).

3.3.2 Avoidance Assays with 10mM $CuCl_2$ After Punicalagin Treatment

Avoidance assays were completed to evaluate the impact of punicalagin treatment on chemoreception of 10mM $CuCl_2$. The average avoidance index of the AD model control CL2122 after treatment was 0.68 ± 0.0725. The average avoidance index of the AD model CL2355 after treatment was 0.60 ± 0.118. Figure 15 shows a comparison of both treatment strains to their baseline avoidance indices. A Welch and Brown-Forsythe ANOVA test was run between treatment and non-treatment solvent controls and found no significant difference. For this reason, solvent control data has been omitted from Figure 15 and can be found in Supplementary Figure 4 (Appendix C).

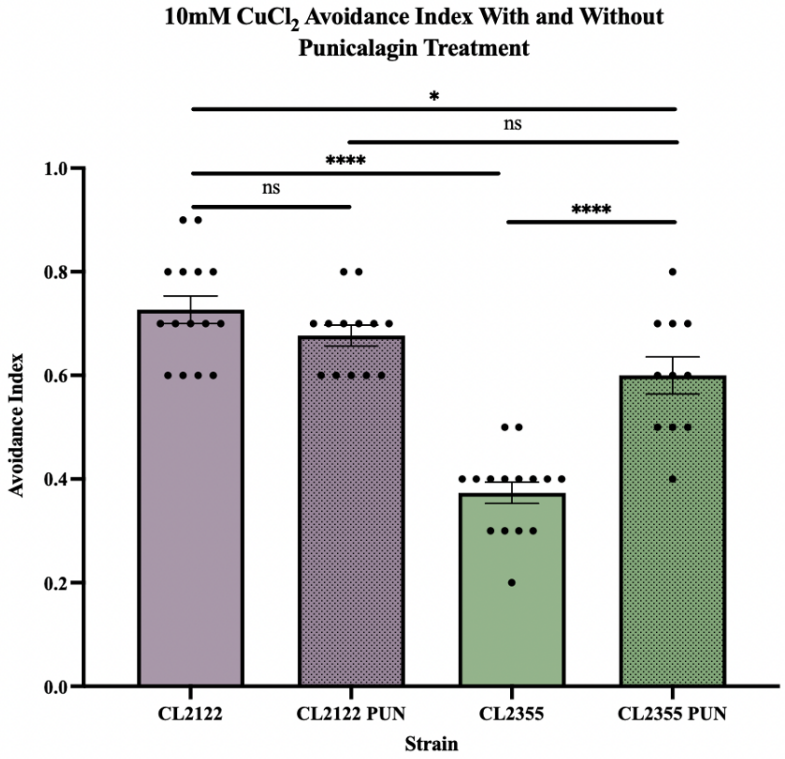

Figure 15. Average avoidance index to 10mM $CuCl_2$ with and without punicalagin treatment (PUN). SC = Solvent control. Error bars are SEM. n ≥ 11. Welch's t-test. “ns” = not significant, *p < 0.05, ****p < 0.0001.

There was a significant increase in avoidance to 10mM $CuCl_2$ when comparing treated to untreated CL2355 strains. Additionally, there was no significant difference in avoidance to 10mM $CuCl_2$ when comparing treated CL2355 to both untreated and treated CL2122 control strains. The treated CL2355 strain did not act significantly different from the controls but did act significantly different than the untreated CL2355 strain. This indicates a full therapeutic effect. The data support that punicalagin treatment improves the deficit in avoidance behavior to 10mM $CuCl_2$.

Punicalagin treatment was shown to increase CL2355 avoidance behavior to both 0.1% SDS and 10mM $CuCl_2$. Since avoidance behavior is indicative of chemoreception, punicalagin treatment was able to improve chemoreception sensitivities of both aversive cues. After treatment, CL2355 exhibited avoidance behavior to both 0.1% SDS and 10mM $CuCl_2$ that was similar to that of controls. This is likely because punicalagin either prevented or decreased the neural damage by Aβ plaques thought to cause decreased sensitivities of aversive cues. With restored sensitivity, the punicalagin treated CL2355 strain could appropriately respond to the aversive chemical stimuli present. They did not need an increase of stimuli to elicit a response as they probably would without treatment.

Since punicalagin is an antioxidant, treatment could have prevented or reduced oxidative stress within the nervous system. Less oxidative stress would have decreased the rate of neurodegeneration. Again, it is unclear in this case if the treatment had neuroprotective versus restorative effects because the worms were treated throughout their life span.

4.0 Conclusions and Future Work

This project first aimed to assess whether the AD model *C. elegans* strain CL2355 exhibited total loss of chemoreception with induction of Aβ plaques, or if the strain retained some sensitivity to aversive stimuli. Through testing the chemoreception of three different aversive stimuli, it was found that the CL2355 strain retained some sensitivity to aversive stimuli. The strain was deficient in avoidance to both 0.1% SDS and 10mM $CuCl_2$ but exhibited robust avoidance behavior to 1M glycerol. This is interesting because all three cues are sensed by the same neuron, the ASH neuron. This implies that Aβ plaque interference causes a deficit in overall chemoreception sensitivity and not in the particular sensation of specific cues. In other words, deficits in CL2355 avoidance behavior seem to be stimuli dose dependent, rather than due

to a total chemoreception loss of certain stimuli. Both 0.1% SDS and 10mM $CuCl_2$ were not strong enough stimuli to stimulate full CL2355 avoidance behavior, unlike 1M glycerol. Future studies could determine the dose required of all three aversive cues to stimulate an avoidance response of CL2355. Based on this study, these doses could be below 1M for glycerol, above 0.1% for SDS and above 10mM for $CuCl_2$. This could be done by establishing a dose response curve for each of the three stimuli. Other well documented aversive cues such as quinine could also be used to test the stimuli dose dependency of CL2355 avoidance behavior.

This study also aimed to test the therapeutic effects of microbiome supplementation and punicalagin extract in improving the deficit in avoidance behavior seen in CL2355. Microbiome supplementation resulted in a partial increase of chemoreception in CL2355. This was seen in testing chemoreception of both 0.1% SDS and 10mM $CuCl_2$ after treatment. There is no confirmation of whether the gut microbiome supplementation helped reconstitute the gut or if it initiated a full healthy recolonization of the gut. It is more likely that a partial reconstitution occurred and this may have translated to the partial improvement of chemoreception deficits seen. For this reason, a study needs to be done characterizing the differences in the gut microbiome between control and CL2355 strains before and after supplementation with CeMbio strains. One possible method would be to isolate the bacteria found in the gut of each *C. elegans* strain and to sequence the 16S rRNA of the samples using multiplexed amplicon sequencing. Multiplexed amplicon sequencing not only allows for bacterial taxonomic classification and running of all samples at the same time, but also tests for relative bacterial abundance (Armanhi et al., 2016).

Punicalagin treatment increased chemoreception to normal levels in CL2355. This was seen in testing chemoreception of both 0.1% SDS and 10mM $CuCl_2$. Treated CL2355 had similar avoidance to that of controls. This is likely because punicalagin restored chemoreception sensitivity by either preventing or treating the neural damage by Aβ plaques. With increased sensitivity, the punicalagin treated CL2355 strain could appropriately respond to the aversive chemical stimuli present. They did not need an increase of stimuli to elicit a response as they probably would without treatment. The findings of this study agree with a previous MQP which also found punicalagin to be an effective treatment in mitigating the behavioral deficit seen in *C. elegans* with Aβ expression (Coyle et al., 2016).

One consideration to be made is that the treatments used in this study were applied to *C. elegans* before and during development. The worms used in avoidance assays were treated from time of hatching to time of assay. This means that they consumed the treatment their entire lives. For this reason, it is possible that the treatments created a neuroprotective effect before the induction of amyloid plaque expression. In other words, they acted as a proactive treatment rather than a retroactive treatment. Although proactive treatments are useful, AD is normally only recognized when physical symptoms are visible after years of underlying biochemical changes. Alzheimer's disease is a progressive neurological disorder, meaning it worsens over time and the highest risk factor for the disease is age. Most patients are seeking retroactive treatment to reverse symptoms of the disease. It may be useful to conduct studies that retroactively treat AD strains by providing treatment after heat shock using both gut microbiome supplementation and punicalagin extract as treatments. These two treatments seem to have potential in interacting with Aβ plaques as seen in this study.

Other future directions for this project include studying the role of sex-bias in the findings above. As mentioned before, women are twice as likely to develop AD than men (Podcasy & Epperson, 2019). It is also interesting to note that the composition of the gut microbiome exhibits sexual dimorphism (Cook et al., 2019). Originally this study aimed to also research the role of sex-bias in the developmet of AD, however efforts to establish a model to do so were unsuccessful (Appendix A; Appendix B). Once a male AD model *C. elegans* strain is established, then the sexually-biased differences in the development of AD and the composition of the gut microbiome and any links between them can be investigated.

5.0 References

Almeida, C., Oliveira, R., Soares, R., & Barata, P. (2020). Influence of gut microbiota dysbiosis on brain function: a systematic review. *Porto biomedical journal*, *5*(2), 1-8. https://doi.org/10.1097/j.pbj.0000000000000059

Altun, Z. F. & Hall, D. H. (2009). *Introduction*. WormAtlas. https://doi.org/10.3908/wormatlas.1.1

Alzheimer's Association. (2020a). *2020 Alzheimer's Disease Facts and Figures.* https://www.alz.org/media/Documents/alzheimers-facts-and-figures_1.pdf

Alzheimer's Association. (2020b, December 28). *Federal Alzheimer's and Dementia Research Funding Reaches $3.1 Billion Annually.* News. https://www.alz.org/news/2020/federal-alzheimers-and-dementia-research-funding-r

Alzheimer's Association. (2021a). *2021 Alzheimer's Disease Facts and Figures.* https://www.alz.org/media/Documents/alzheimers-facts-and-figures.pdf

Alzheimer's Association. (2021b). *Younger/Early-Onset Alzheimer's.* What is Alzheimer's Disease? https://www.alz.org/alzheimers-dementia/what-is-alzheimers/younger-early-onset

Armanhi, J., de Souza, R., de Araújo, L., ... & Arruda, P. Multiplex amplicon sequencing for microbe identification in community-based culture collections. *Sci Rep* 6, 29543 (2016). https://doi.org/10.1038/srep29543

Awasthi, M., Singh, S., Pandey, V. P., & Dwivedi, U. N. (2016). Alzheimer's disease: An overview of amyloid beta dependent pathogenesis and its therapeutic implications along with in silico approaches emphasizing the role of natural products. *Journal of the neurological sciences*, *361*, 256-271. https://doi.org/10.1016/j.jns.2016.01.008

Beltrán-Sánchez, H., Soneji, S., & Crimmins, E. M. (2015). Past, Present, and Future of Healthy Life Expectancy. *Cold Spring Harbor perspectives in medicine*, *5*(11), a025957. https://doi.org/10.1101/cshperspect.a025957

Berg, M., Stenuit, B., Ho, J., Wang, A., Parke, C., Knight, M., ... & Shapira, M. (2016). Assembly of the Caenorhabditis elegans gut microbiota from diverse soil microbial environments. *The ISME journal*, *10*(8), 1998-2009. https://doi.org/10.1038/ismej.2015.253

Bull, M. J., & Plummer, N. T. (2014). Part 1: The Human Gut Microbiome in Health and Disease. *Integrative medicine (Encinitas, Calif.)*, *13*(6), 17–22.

Carabotti, M., Scirocco, A., Maselli, M. A., & Severi, C. (2015). The gut-brain axis: interactions between enteric microbiota, central and enteric nervous systems. *Annals of gastroenterology*, *28*(2), 203–209. https://www.ncbi.nlm.nih.gov/pmc/articles/PMC4367209/

Centers for Disease Control and Prevention. (2019). *About Underlying Cause of Death, 1999-2019*. CDC Wonder. https://wonder.cdc.gov/ucd-icd10.html

Centers for Disease Control and Prevention. (2021a). *Leading Causes of Death*. National Center for Health Statistics. https://www.cdc.gov/nchs/fastats/leading-causes-of-death.htm

Centers for Disease Control and Prevention. (2021b). *Alzheimer's Disease.* Disease or Condition of the Week. https://www.cdc.gov/dotw/alzheimers/index.html

Cheignon, C., Tomas, M., Bonnefont-Rousselot, D., Faller, P., Hureau, C., & Collin, F. (2018). Oxidative stress and the amyloid beta peptide in Alzheimer's disease. *Redox biology*, *14*, 450-464. https://doi.org/10.1016/j.redox.2017.10.014

Chen, X., Barclay, J.W., Burgoyne, R.D. & Morgan, A. (2015). Using *C. elegans* to discover therapeutic compounds for ageing-associated neurodegenerative diseases. *Chemistry Central Journal*, 9(1), 65. https://doi.org/10.1186/s13065-015-0143-y

Christen-Zaech, S., Kraftsik, R., Pillevuit, O., Kiraly, M., Martins, R., Khalili, K., & Miklossy, J. (2003). Early olfactory involvement in Alzheimer's disease. *The Canadian journal of neurological sciences. Le journal canadien des sciences neurologiques*, *30*(1), 20–25. https://doi.org/10.1017/s0317167100002389

Chute, C. (2018). *Decoding Neural Circuits Modulating Behavioral Responses to Aversive Social Cues*. Worcester Polytechnic Institute.

Consedine, T., McNeill, N., & Randle, L. (2018). *Establishing a Connection between Alzheimer's Disease and Cellular Energy Transduction.* Worcester Polytechnic Institute.

Cook, S. J., Jarrell, T. A., Brittin, C. A., ... & Emmons, S. W. Whole-animal connectomes of both Caenorhabditis elegans sexes. Nature 571, 63–71 (2019). https://doi.org/10.1038/s41586-019-1352-7

Corsi, A. K., Wightman, B., & Chalfie, M. (2015). *A Transparent window into biology: A primer on Caenorhabditis elegans*. WormBook. doi/10.1895/wormbook.1.177.1

Coyle, V., Nikolaki, V., & Ong, F. (2016). *The Effects of Punicalagin and Tannic Acid on Caenorhabditis elegans Models of Alzheimer's Disease.* Worcester Polytechnic Institute.

De-Paula, V. J., Radanovic, M., Diniz, B. S., & Forlenza, O. V. (2012). Alzheimer's disease. *Sub-cellular biochemistry*, 65, 329–352. https://doi.org/10.1007/978-94-007-5416-4_14

Dirksen, P., Assié, A., Zimmermann, J., Zhang, F., Tietje, A. M., Marsh, S. A., ... & Samuel, B. S. (2020). CeMbio-The Caenorhabditis elegans microbiome resource. *G3: Genes, Genomes, Genetics*, *10*(9), 3025-3039. https://doi.org/10.1534/g3.120.401309

Dirksen, P., Marsh, S. A., Braker, I., Heitland, N., Wagner, S., Nakad, R., ... & Schulenburg, H. (2016). The native microbiome of the nematode Caenorhabditis elegans: gateway to a new host-microbiome model. *BMC biology*, *14*(1), 1-16. https://doi.org/10.1186/s12915-016-0258-1

Friedland, R. P., & Chapman, M. R. (2017). The role of microbial amyloid in neurodegeneration. *PLoS pathogens*, *13*(12), e1006654. https://doi.org/10.1371/journal.ppat.1006654

Gella, A., & Durany, N. (2009). Oxidative stress in Alzheimer disease. *Cell adhesion & migration*, *3*(1), 88–93. https://doi.org/10.4161/cam.3.1.7402

Hardy, J., & Selkoe, D. J. (2002). The amyloid hypothesis of Alzheimer's disease: progress and problems on the road to therapeutics. *Science (New York, N.Y.)*, *297*(5580), 353–356. https://doi.org/10.1126/science.1072994

Hart, A. C. (2006). *Behavior*. WormBook. doi/10.1895/wormbook.1.87.1

Hart, A. C., & Chao, M., Y. (2010). *Chapter 1: From Odors to Behaviors in Caenorhabditis elegans*. The Neurobiology of Olfaction. https://www.ncbi.nlm.nih.gov/books/NBK55983/

Heneka, M. T., Carson, M. J., El Khoury, J., Landreth, G. E., Brosseron, F., Feinstein, D. L., ... & Kummer, M. P. (2015). Neuroinflammation in Alzheimer's disease. *The Lancet. Neurology*, *14*(4), 388–405. https://doi.org/10.1016/S1474-4422(15)70016-5

Hilliard, M. A., Bargmann, C. I., & Bazzicalupo, P. (2002). C. elegans responds to chemical repellents by integrating sensory inputs from the head and the tail. *Current Biology*, *12*(9), 730-734. https://doi.org/10.1016/s0960-9822(02)00813-8

Hilliard, M. A., Bergamasco, C., Arbucci, S., Plasterk, R. H., & Bazzicalupo, P. (2004). Worms taste bitter: ASH neurons, QUI-1, GPA-3 and ODR-3 mediate quinine avoidance in

Caenorhabditis elegans. *The EMBO journal*, *23*(5), 1101–1111. https://doi.org/10.1038/sj.emboj.7600107

Huang, W. J., Zhang, X., & Chen, W. W. (2016). Role of oxidative stress in Alzheimer's disease. *Biomedical reports*, *4*(5), 519–522. https://doi.org/10.3892/br.2016.630

Jašarević, E., Morrison, K. E., & Bale, T. L. (2016). Sex differences in the gut microbiome-brain axis across the lifespan. *Philosophical transactions of the Royal Society of London. Series B, Biological sciences*, *371*(1688), 20150122. https://doi.org/10.1098/rstb.2015.0122

Kaletta, T., & Hengartner, M. O. (2006). Finding function in novel targets: C. elegans as a model organism. *Nature reviews Drug discovery*, *5*(5), 387-399. https://doi.org/10.1038/nrd2031

Kim, Y. E., Hwang, C. J., Lee, H. P., Kim, C. S., Son, D. J., Ham, Y. W., ... & Hong, J. T. (2017). Inhibitory effect of punicalagin on lipopolysaccharide-induced neuroinflammation, oxidative stress and memory impairment via inhibition of nuclear factor-kappaB. *Neuropharmacology*, *117*, 21-32. https://doi.org/10.1016/j.neuropharm.2017.01.025

Kim, Y. K., & Shin, C. (2018). The Microbiota-Gut-Brain Axis in Neuropsychiatric Disorders: Pathophysiological Mechanisms and Novel Treatments. *Current neuropharmacology*, *16*(5), 559–573. https://doi.org/10.2174/1570159X15666170915141036

Knupfer, L., & Spiegel, R. (1986). Differences in olfactory test performance between normal aged, Alzheimer and vascular type dementia individuals. *International Journal of Geriatric Psychiatry*, *1*(1), 3-14. https://doi.org/10.1002/gps.930010103

Kowalski, K., & Mulak, A. (2019). Brain-Gut-Microbiota Axis in Alzheimer's Disease. *Journal of neurogastroenterology and motility*, *25*(1), 48–60. https://doi.org/10.5056/jnm18087

Link, C. D. (2005). Invertebrate models of Alzheimer's disease. *Genes, Brain and Behavior*, *4*(3), 147-156. https://doi.org/10.1111/j.1601-183X.2004.00105.x

Markaki, M., & Tavernarakis, N. (2010). Modeling human diseases in Caenorhabditis elegans. *Biotechnology journal*, *5*(12), 1261-1276. https://doi.org/10.1002/biot.201000183

Mielke, M. M., Vemuri, P., & Rocca, W. A. (2014). Clinical epidemiology of Alzheimer's disease: assessing sex and gender differences. *Clinical epidemiology*, *6*, 37–48. https://doi.org/10.2147/CLEP.S37929

Molina-García, L., Lloret-Fernández, C., Cook, S. J., Kim, B., Bonnington, R. C., Sammut, M., ... & Poole, R. J. (2020). Direct glia-to-neuron transdifferentiation gives rise to a pair of

male-specific neurons that ensure nimble male mating. *Elife*, *9*, e48361. https://doi.org/10.7554/eLife.48361

Mullard, A. (2021, June 29). *Controversial Alzheimer's drug approval could affect other diseases.* Nature News. https://www.nature.com/articles/d41586-021-01763-9

National Institutes of Health. (2020). APP gene: amyloid beta precursor protein. U.S. National Library of Medicine. https://ghr.nlm.nih.gov/gene/APP#conditions

National Institute on Aging. (2017). *What Happens to the Brain in Alzheimer's Disease?* Causes of Alzheimer's Disease. https://www.nia.nih.gov/health/what-happens-brain-alzheimers-disease

National Institute on Aging. (2021). *How Is Alzheimer's Disease Treated?* Treatment of Alzheimer's Disease. https://www.nia.nih.gov/health/how-alzheimers-disease-treated

Olajide, O. A., Kumar, A., Velagapudi, R., Okorji, U. P., & Fiebich, B. L. (2014). Punicalagin inhibits neuroinflammation in LPS‐activated rat primary microglia. *Molecular nutrition & food research*, *58*(9), 1843-1851. https://doi.org/10.1002/mnfr.201400163

Podcasy, J. L., & Epperson, C. N. (2016). Considering sex and gender in Alzheimer disease and other dementias. *Dialogues in clinical neuroscience*, *18*(4), 437–446. https://doi.org/10.31887/DCNS.2016.18.4/cepperson

Reitz, C., Brayne, C., & Mayeux, R. (2011). Epidemiology of Alzheimer disease. *Nature reviews. Neurology*, *7*(3), 137–152. https://doi.org/10.1038/nrneurol.2011.2

Rocca, W. A., Mielke, M. M., Vemuri, P., & Miller, V. M. (2014). Sex and gender differences in the causes of dementia: a narrative review. *Maturitas*, *79*(2), 196–201. https://doi.org/10.1016/j.maturitas.2014.05.008

Saji, N., Murotani, K., Hisada, T., Kunihiro, T., Tsuduki, T., Sugimoto, T., ... & Sakurai, T. (2020). Relationship between dementia and gut microbiome-associated metabolites: a cross-sectional study in Japan. *Scientific reports*, *10*(1), 1-11.

Sambongi, Y., Nagae, T., Liu, Y., Yoshimizu, T., Takeda, K., Wada, Y., & Futai, M. (1999). Sensing of cadmium and copper ions by externally exposed ADL, ASE, and ASH neurons elicits avoidance response in Caenorhabditis elegans. *NeuroReport*, *10*(4), 753-757. https://doi.org/10.1097/00001756-199903170-00017

Samuel, B. S., Rowedder, H., Braendle, C., Félix, M. A., & Ruvkun, G. (2016). Caenorhabditis elegans responses to bacteria from its natural habitats. *Proceedings of the National Academy of Sciences*, *113*(27), E3941-E3949. https://doi.org/10.1073/pnas.1607183113

Tang, Y. P., & Gershon, E. S. (2003). Genetic studies in Alzheimer's disease. *Dialogues in clinical neuroscience*, *5*(1), 17–26. https://doi.org/10.31887/DCNS.2003.5.1/yptang

Tkalčić, M., Spasić, N., Ivanković, M., Pokrajac-Bulian, A., & Bosanac, D. (2011). Odor identification and cognitive abilities in Alzheimer's disease. *Translational Neuroscience*, *2*(3), 233-240. https://doi.org/10.2478/s13380-011-0026-1

U.S. Food & Drug Administration. (2021). *Aducanumab (marketed as Aduhelm) Information*. Postmarket Drug Safety Information for Patients and Providers. https://www.fda.gov/drugs/postmarket-drug-safety-information-patients-and-providers/aducanumab-marketed-aduhelm-information

Vogt, N. M., Kerby, R. L., Dill-McFarland, K. A., Harding, S. J., Merluzzi, A. P., Johnson, S. C., Carlsson, C. M., Asthana, S., Zetterberg, H., Blennow, K., Bendlin, B. B., & Rey, F. E. (2017). Gut microbiome alterations in Alzheimer's disease. *Scientific reports*, *7*(1), 13537. https://doi.org/10.1038/s41598-017-13601-y

Wu, Y., & Luo, Y. (2005). Transgenic C. elegans as a model in Alzheimer's research. *Current Alzheimer Research*, *2*(1), 37-45. https://doi.org/10.2174/1567205052772768

Zhan, X., Stamova, B., & Sharp, F. R. (2018). Lipopolysaccharide Associates with Amyloid Plaques, Neurons and Oligodendrocytes in Alzheimer's Disease Brain: A Review. *Frontiers in aging neuroscience*, *10*, 42. https://doi.org/10.3389/fnagi.2018.00042

Zhang, F., Berg, M., Dierking, K., Félix, M. A., Shapira, M., Samuel, B. S., & Schulenburg, H. (2017). Caenorhabditis elegans as a model for microbiome research. *Frontiers in Microbiology*, *8*, 485. https://doi.org/10.3389/fmicb.2017.00485

Zhang, R., Miller, R. G., Gascon, R., Champion, S., Katz, J., Lancero, M., Narvaez, A., Honrada, R., Ruvalcaba, D., & McGrath, M. S. (2009). Circulating endotoxin and systemic immune activation in sporadic amyotrophic lateral sclerosis (sALS). *Journal of neuroimmunology*, *206*(1-2), 121–124. https://doi.org/10.1016/j.jneuroim.2008.09.017

Zheng, S. Q., Ding, A. J., Li, G. P., Wu, G. S., & Luo, H. R. (2013). Drug absorption efficiency in Caenorhabditis elegans delivered by different methods. *PloS one*, *8*(2), e56877. https://doi.org/10.1371/journal.pone.0056877

Zhou, Y., Smith, D., Leong, B. J., Brännström, K., Almqvist, F., & Chapman, M. R. (2012). Promiscuous cross-seeding between bacterial amyloids promotes interspecies biofilms. *The Journal of biological chemistry*, *287*(42), 35092–35103. https://doi.org/10.1074/jbc.M112.383737

Zou, Y. M., Lu, D., Liu, L. P., Zhang, H. H., & Zhou, Y. Y. (2016). Olfactory dysfunction in Alzheimer's disease. *Neuropsychiatric disease and treatment*, *12*, 869–875. https://doi.org/10.2147/NDT.S104886

Appendix A: Supplementary Methods

CL2355 x *him-5* Cross

A cross between the CL2355 and *him-5* strains was attempted in order to create a male AD model *C. elegans* strain. In theory, this strain could be used to study sex specific differences in the development of Alzheimer's disease. To start the cross, 5 plates were made with 1 CL2355 hermaphrodite and 8 or more *him-5* males. The parental generation cross plates were labeled P1 through P5 and were placed at 15-16℃ until the F1 generation was at the L4 stage. Cross plates were considered successful if they had over 20% fluorescent males (a genetic marker for the Aβ gene). The number of fluorescent males for each progeny plate was recorded.

Each successful plate was singled out into 10 future generation plates if possible. Successful plates were singled by placing 1 fluorescent L4 hermaphrodite onto a freshly seeded OP50 plate. Hermaphrodites were allowed to self fertilize and lay eggs at 15-16℃ until the F2 generation was at the L4 stage. The process of identifying and passing successful plates was then repeated. Each generation was numbered with their corresponding generation number and a unique identifier to trace back to its parental lineage. Generations were continued until all 10 singled plates from a successful plate were also successful. The cross was discontinued if fluorescent males were lost.

Appendix B: Supplementary Results

CL2355 x *him-5* Cross

The CL2355 x *him-5* cross was attempted on two occasions and was unsuccessful both times. Attempt 1 was brought to the 9th generation and was assumed complete after all singled progeny plates had fluorescent males. This new strain was named JSR152. Unfortunately, within a generation of passing JSR152 the males with fluorescence were lost. Attempt 2 was brought to the 6th generation and was discontinued after males with fluorescence were lost again. It was found that the first generation of the cross always produced fluorescent males. In subsequent generations, the percentage of fluorescent males steadily decreased and would eventually be lost. There may be an unanticipated crossover event during meiosis. The *him-5* mutation and CL2355 gene construct are located on different chromosomes, so a crossover event was not anticipated. Both genes are homozygous recessive, so it is possible that the CL2355 x *him-5* cross cannot be successful without a back cross with *him-5* hermaphrodites after F1.

Appendix C: Supplementary Figures

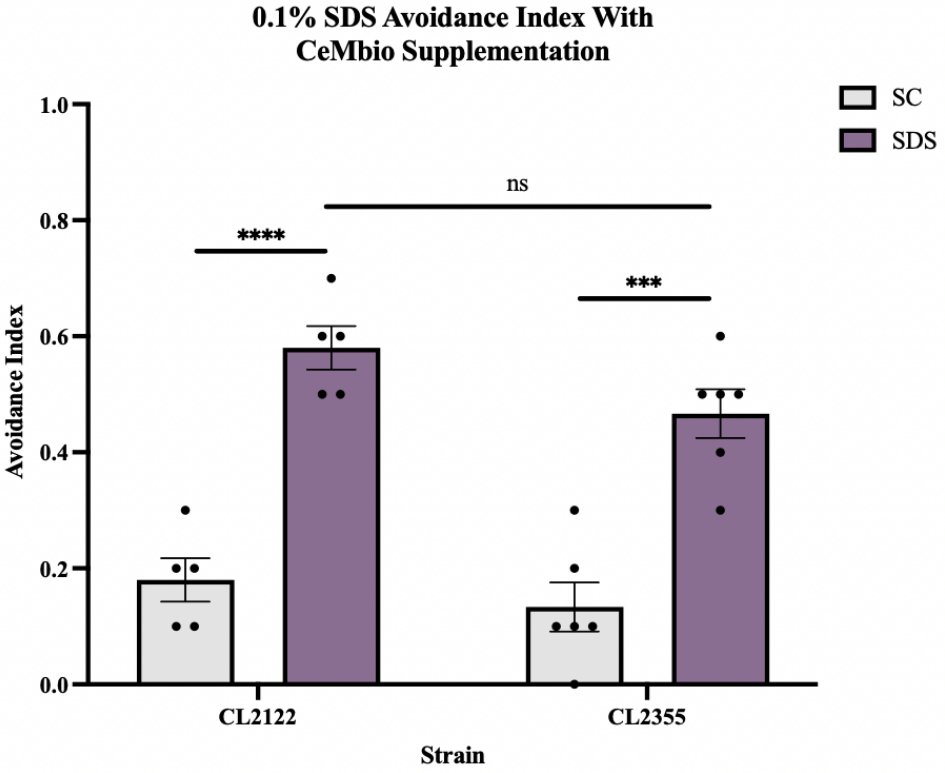

Supplementary Figure 1. Average avoidance index to 0.1% SDS with gut microbiome supplementation with CeMbio strains. SC = Solvent control. Error bars are SEM. n ≥ 5. Welch's t-test. “ns” = not significant, ***p < 0.001, ****p < 0.0001

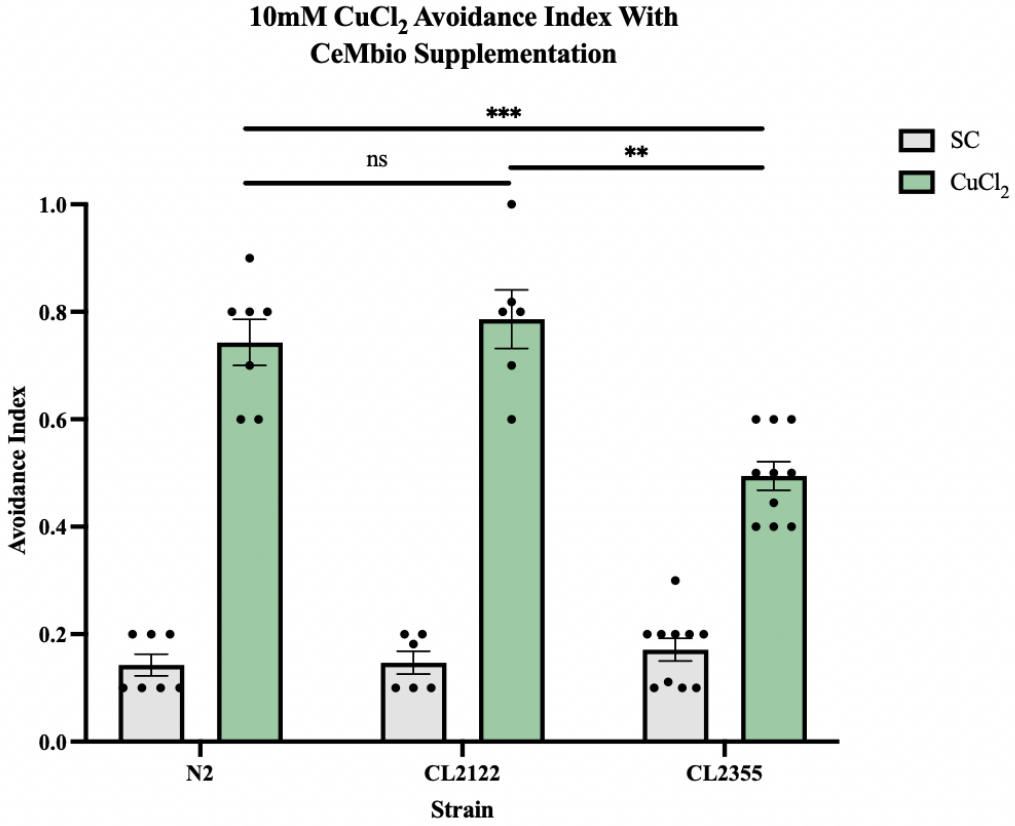

Supplementary Figure 2. Average avoidance index to 10mM $CuCl_2$ with gut microbiome supplementation with CeMbio strains. SC = Solvent control. Error bars are SEM. $n \geq 6$. Welch's t-test. "ns" = not significant, $^{**}p < 0.01$, $^{***}p < 0.001$

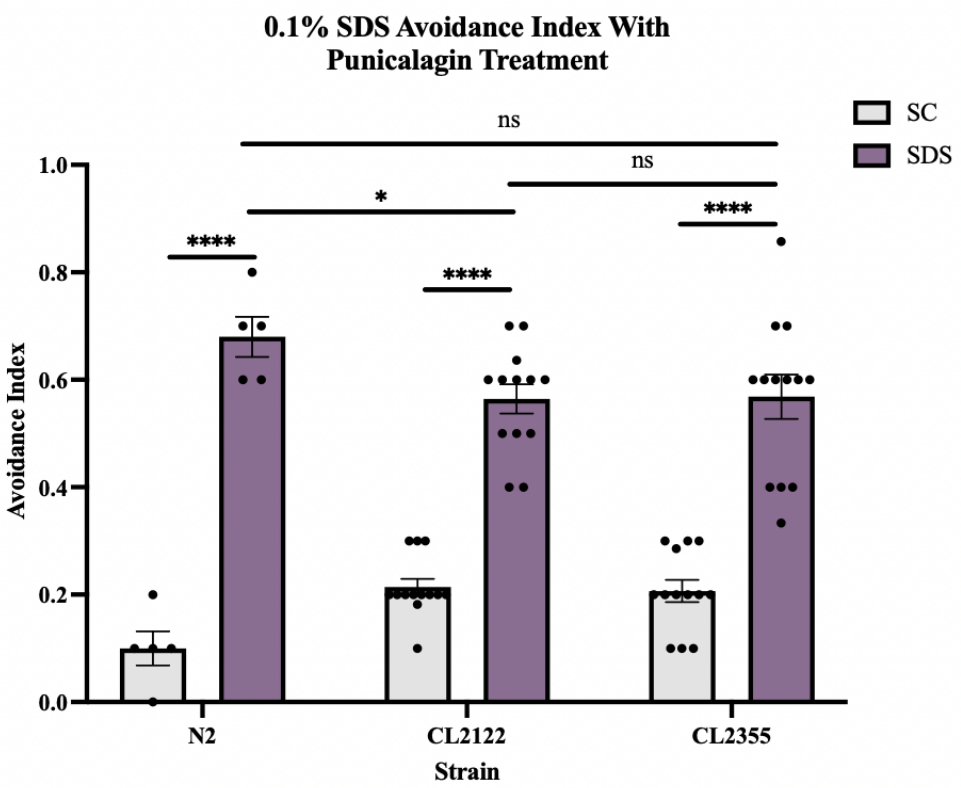

Supplementary Figure 3. Average avoidance index to 0.1% SDS with punicalagin treatment. SC = Solvent control. Error bars are SEM. n ≥ 5. Welch's t-test. “ns” = not significant, *p < 0.05, ****p < 0.0001

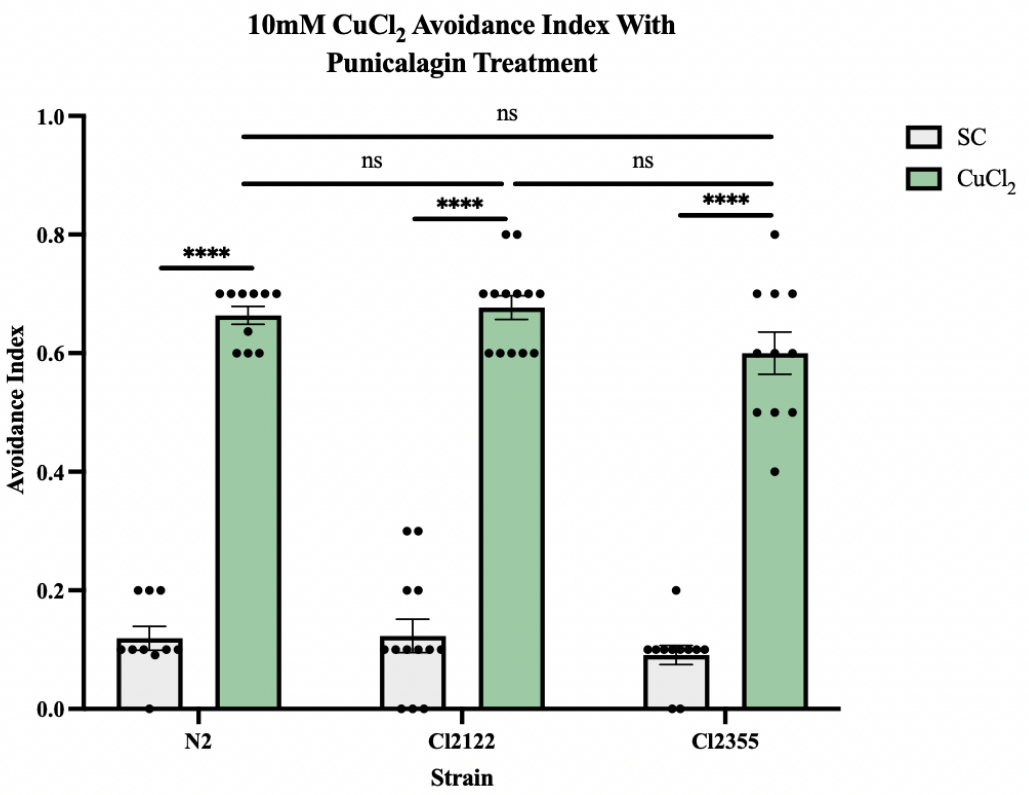

Supplementary Figure 4. Average avoidance index to 10mM $CuCl_2$ with punicalagin treatment. SC = Solvent control. Error bars are SEM. n ≥ 10. Welch's t-test. "ns" = not significant, ****p < 0.0001

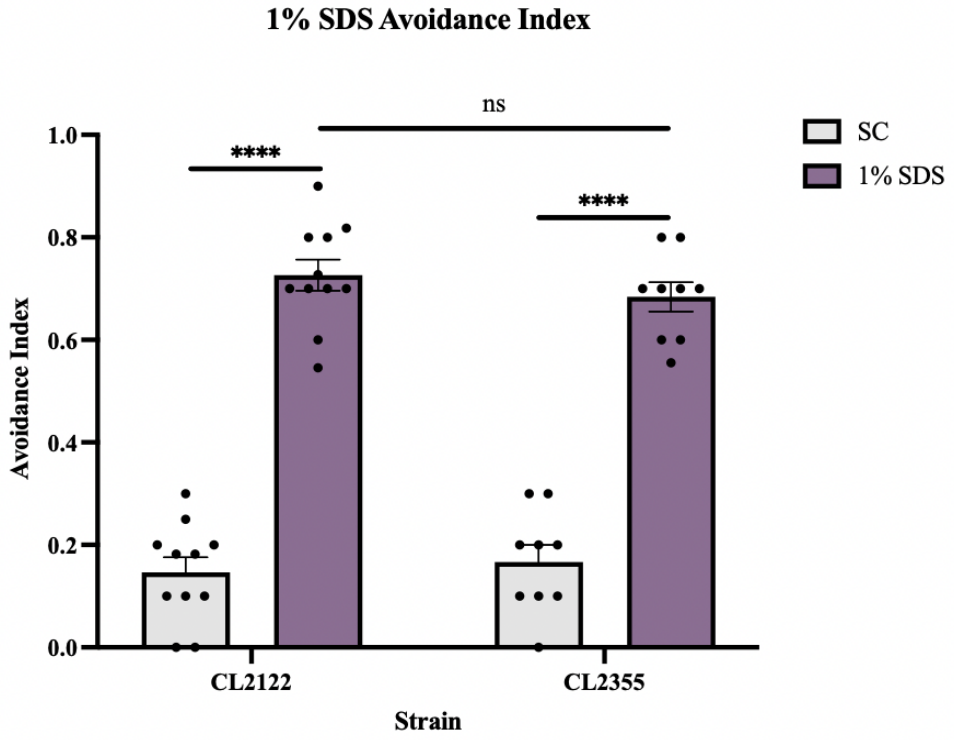

Supplementary Figure 5. Average avoidance index to 1% SDS. SC = Solvent control. Error bars are SEM. n ≥ 9. Welch's t-test. “ns” = not significant, ****p < 0.0001